School of Multidisciplinary Engineering

Center for Materials Engineering

Study on Nickel Nitride Core Nitrogen Doped Carbon Shell Structure as Electrocatalyst for Oxygen Evolution Reaction

by Teferi Mekit

Advisor: - Dr. Sintayehu Nibret

The Thesis Submitted to Center for Materials Engineering in Partial Fulfillment of the Requirements for the Degree of Masters of Science in Materials Engineering

Nov, 2023
Addis Ababa university, Addis Ababa, Ethiopia

CANDIDATE'S DECLARATION

I hereby declare the work which is being presented in the thesis, entitled novel nickel nitride core nitrogen doped carbon shell structure for oxygen evolution reaction in partial fulfilment of the requirement for award of the degree of masters of science in materials engineering and submitted to Center for Materials Engineering, School of Multidisciplinary Engineering, Addis Ababa Institute of Technology, Addis Ababa University is an original pieces of research work under guidance of Dr. Sintayehu Nibret. The matters in this thesis is my original work and has not been presented for a degree in any other University and that all sources of materials used for the thesis have been duly acknowledged.

Teferi Mekit Dillo

Candidate_____ _____ _____

December 2022 Signature Date

This thesis is submitted for examination with my approval as an advisor of the candidate.

Dr. Sintayehu Nibret _____ _____

Advisor Signature Date

Center for Materials Engineering (CME)School of Multi-Disciplinary Engineering Addis Ababa Institute of Technology

Study on Nickel Nitride Core Nitrogen Doped Carbon Shell Structure as Electrocatalyst for Oxygen Evolution Reaction

By: - Teferi Mekit

Advisor: - Dr. Sintayehu Nibret

BOARD OF EXAMINERS:

Dr. Tesfay Refera	_____	_____
External Examiner	Signature	Date
Dr. George Alene	_____	_____
Internal examiner	Signature	Date
Dr. Sintayehu Nibret	_____	_____
Chairman and advisor	Signature	Date

ACKNOWLEDGEMENT

In advance I would give sincerely appreciation and great thanks to my advisor Dr. Sintayehu Nibret for all his decisive leadership quality, respecting of others opinion, being committed to do in cooperate continuous follow up from the beginning, leading to the right direction, guidance, suggestions, encouragements, valuable comments in general for all his all-inclusive support for the realization of this research.

I would like to express my heartfelt gratitude to the **Chemical and Construction Inputs Industry Development Institute** for their generous partial sponsorship of my MSc studies. Their support has been instrumental in my academic journey, enabling me to focus on my research and academic development without the burden of financial constraints.

Additionally, I wish to acknowledge the **Addis Ababa Institute of Technology (AAiT)**, particularly the **Center for Materials Engineering**. I am especially thankful to **Dr. Sintayehu Nibret** for granting me access to crucial raw data from the experimental studies conducted at the **School of Advanced Materials Science and Engineering** at **Sungkyunkwan University**, South Korea. This data has been vital for my analysis and interpretation, allowing me to engage deeply with the subject matter and contribute meaningfully to the field.

Finally, I extend my deepest appreciation to my beloved brothers for their unwavering support and encouragement in various aspects of my life. Their presence has been a source of strength throughout this journey, providing me with the motivation and resilience needed to overcome challenges and pursue my academic goals.

ABSTRACT

The oxygen evolution reaction (OER) is vital for electrochemical water splitting, enabling a viable, ecologically positive, and sustainable approach for hydrogen energy production. Due to the high costs and restricted availability of noble metal catalysts, transition metal non-oxides such as nitrides, phosphides, selenides, and sulphides present potential alternatives that can give strong OER activity and durability. The OER mechanism is intrinsically sluggish, needing large energy to break hydrogen bonds and produce O-O bonds. Additionally, the high binding energies of critical kinetic intermediates (*O, *OH, and *OOH)—further contribute to the sluggish reaction rates. Nickel nitride (Ni_3N) has gained great attention because of its substantial potential, low cost, and ease of fabrication. Its mechanical stability is strengthened when enclosed in a nitrogen-doped carbon electrocatalyst architecture, Ni_3N@NC; hence, the catalyst can bear the pressures of electrochemical reactions without showing major changes in structure or loss of active sites. The present architecture offers an improvement in charge transfer through void space between a nickel core and a nitrogen-doped carbon shell while introducing additional active sites for catalytic processes. A nitrogen-doped carbon shell with a porous structure facilitates mass transport due to better dispersion of reactants and products. The core-shell samples of Ni_3N@NC were prepared by coating nickel metal with polydopamine using the pH-induced oxidative polymerization in alkaline solution (pH 8.5), then acid etching of the core was performed to introduce a void space between the core and an outer PDA-derived NC shell. In the process, crystalline phases, surface morphologies, microstructures, and composition were characterized using different methods like XRD, FE-SEM, TEM, Raman spectroscopy, and XPS to describe Ni_3N@NC. Accordingly, the electrocatalytic activity of prepared samples was investigated both for OER and hydrogen evolution reactions. It is viewed that the overpotential of the OER electrocatalyst Ni_3N@NC/24hr was 292.8 mV at a current density of 10 mA cm^{-2}, while the Tafel slope was 110.68 mV dec^{-1}. This further confirmed its catalytic nature towards OER and established its potential in various sustainable hydrogen production applications.

Key words: water splitting, core shell structure, electrocatalyst, nickel nitride, nitrogen doped carbon, oxygen evolution reaction, hydrogen evolution reaction

Table of Contents

page

LIST OF FIGURES

LIST OF TABLES

ABBREVIATIONS

CP	Chronopotentiometry
Ni_3N@NC	Nickel Nitride Core–Nitrogen Doped Carbon Shell
CV	Cyclic Voltammetry
EDX	Energy Dispersive X-Ray Spectroscopy
HER	Hydrogen Evolution Reaction
HR-TEM	High Resolution Transmission Electron Microscopy
LSV	Linear Sweep Voltammetry
OER	Oxygen Evolution Reaction
PDA	Polydopamine
STEM	Scanning Transmission Electron Microscopy
TEM	Transmission Electron Microscopy
TMNs	Transition Metal Nitrides
XPS	X-Ray Photoelectron Spectroscopy
XRD	X-ray Powder Diffraction

1. INTRODUCTION

1.1 Background

The best way to guarantee a solution to the global energy crisis and a shortage of ecologically friendly energy sources is to acquire and distribute unsearchable riches of renewable, sustainable, clean, and highly efficient energy[1,2]. In response to the ever-growing demand for clean, efficient, and pollution-free energy, significant interest has been established in alternative energy sources from available resources [3]. Scientists and technologists are evolving at a quick pace by comprehending the underlying processes and taking pre-usage measures. Among the technologies under extensive development, few have proved to be particularly promising, especially electrocatalytic water splitting. This technique has emerged as one of the most adequate modes of sustainable hydrogen production to alleviate the global energy dilemma[2,4,5]. This electrolysis process offers pay of such as mild reaction conditions, high-purity hydrogen generation, and renewable production [6].

Among these, electrolysis represents an important technology in synthesizing hydrogen through two major half reactions: the hydrogen evolution reaction at the cathode and the oxygen evolution reaction at the anode. As essence, HER is much more favorable than OER; however, the kinetic lags in OER are intrinsically greater. This sluggishness is mostly related to the high overpotentials required to drive the reaction, which might limit overall efficiency in water splitting systems. The OER is thermodynamically unfavorable and consists of four-electron transfer process; consequently, large energy inputs are necessary to achieve practical reaction rates. Due to this intricacy, this generally constitutes a bottleneck in the process of electrolysis, where the performance scale of the complete system is constrained by OER kinetics. Therefore, active yet inexpensive electrocatalysts for boosting OER performance are increasingly needed [1,7].

Novel metal oxides such as RuO_2 and IrO_2 are considered state-of-the-art catalysts for both the OER and HER due to their excellent catalytic activity and stability [8]. These catalysts are capable of enabling the essential processes that have to occur in order to achieve efficient water splitting a viable strategy toward the production of sustainable hydrogen. However, despite their outstanding performance, these noble metal catalysts confront substantial hurdles relating to cost-effectiveness,

stability, and scalability [9]. The rarity and expensive price of noble metals hinder their broad implementation in large-scale energy systems [4].

Lately research has focused on developing noble metal-free catalysts and enhancing existing noble metal catalysts for efficient water splitting and ammonia synthesis. Surface and interface engineering strategies have been employed to improve the performance of non-noble metal catalysts for (OER), (HER), and overall water splitting[10].

In order to balance activity and stability, metal catalysts have recently been improved using a variety of strategies, including but not limited to altering their composition and structure [11]. Recent studies have concentrated on developing active catalysts for water splitting and hydrogen evolution by encasing nickel-based nanoparticles in carbon shells doped with nitrogen. Synergistic effects of the nickel core and the N-C shell which alter electronic structures and increase active sites have shown increased electrocatalytic activity. Because of the low overpotentials for both HER and OER, the N-C shell provides further protection while improving electron transit [12,13]. In this study, a novel and non-noble electrode material, Ni_3N@NC, is designed and developed to improve water splitting for the OER. A simple polydopamine (PDA) coating and annealing method produced the novel electrocatalyst composed of N-doped carbon (NC) shell which encloses a nickel nitride core (Ni_3N). The study presents that the Ni_3N@NC acts as an efficient catalyst for both OER and HER. In such a way, the proposed core-shell structure is positioned as a feasible non-noble electrocatalyst material for water splitting since it exhibits better and comparable OER activity in comparison with nickel-based electrocatalysts.

1.2 Statement of the Problem

The OER is a critical process in various energy conversion and storage technologies, including water splitting, metal-air batteries, and regenerative fuel cells. However, the efficiency of OER is significantly hindered by the high overpotential required to drive the reaction, which is primarily due to the sluggish kinetics of the four-electron transfer process.

Traditionally, noble metal-based electrocatalysts, such as iridium oxide (IrO_2) and ruthenium oxide (RuO_2), have been employed to enhance the OER activity due to their excellent catalytic performance and stability. Nevertheless, the high cost and scarcity of these noble metals pose substantial challenges for their widespread application in large-scale energy systems. In addition,

susceptibility to structural collapse in acidic conditions reduces the active sites of the materials and weakens their performance [9]. Moreover, intrinsically reacted mechanisms—especially in relation to the OER—are so complex that predicting catalytic behavior becomes difficult[14,15].

In their emergence, transition metals like Ni, Co, Mn, and Cu became beneficial alternatives owing to their abundance, low cost, and tunable properties. Among the nickel-based catalysts, Ni_3N and metallic nickel revealed excellent performance for both HER and OER in alkaline conditions. These catalysts still face some problems with sluggish kinetics and the high overpotentials required to drive the reactions, which eventually limit their overall efficiency in water-splitting systems [1,7]. Accordingly, incorporating transition metals based materials such as Ni_3N into an N-C matrix opens a new window of opportunity toward improved electrocatalytic activities.

Therefore, the development of efficient and stable non-noble electrocatalysts for OER is crucial for advancing sustainable energy technologies and reducing our reliance on precious metals. Addressing this problem will not only contribute to the economic feasibility of renewable energy systems but also promote the adoption of environmentally friendly and scalable solutions for energy conversion and storage.

1.3 Objectives

1.3.1 General Objective

The general objective of this study is synthesis of a unique nickel nitride core and nitrogen doped carbon shell structure electrocatalyst for water splitting specifically for OER.

1.3.2 Specific Objectives

- Designing and preparation of a nickel nitride core-nitrogen doped carbon shell structure (Ni_3N@NC) electrocatalyst.
- To investigate the overpotential of the as-prepared Ni_3N@NC for OER and HER.
- To study series and charge transfer resistance of the best electrocatalyst for OER.
- To investigate the stability of the best electrocatalyst for OER.

1.4 Scope of the study

The work of this thesis is focused on design and fabrication of a novel electrocatalyst, Ni_3N@NC, by morphology tuning to get a core shell structure and investigation of the electrochemical properties of the catalysts for OER and HER while giving more emphasis to OER.

1.5 Significance of the Study

Researches on synthesizing, characterizing and measuring performance of an electrocatalyst with the ultimate goal of hydrogen production as an environmentally friendly energy is growing at a fast rate. Alongside the development of electrocatalysts, preparation of novel structures from cheaper materials is important on the journey of electrocatalyst improvement. Therefore, this study plays its vital role by revealing the significance of morphology tuning of non-noble electrode materials for water splitting to get a better catalytic activity and stability. In addition, the research contributes a simplified and novel method to prepare a core shell structure for water splitting from non-noble transition metals based electrocatalyst.

2. LITERATURE REVIEW

2.1 Introduction

With the rapid consumption of fossil fuel and its adverse effect on eco-friendly, it is crucial to construct cost-effective and clean energy technologies[16] unpolluted and renewable energy resource to replace fossil fuels, hydrogen has paying attention. Splitting of water is amongst accepted as an ideal way to convert in to hydrogen fuel. However, anodic of the half reactions in water splitting, OER is kinetically very sluggish due to deceleration by manifold steps of proton-coupled electron shift and intensified energy impede enquired for both O-H bond splitting and O-O bond formation [17].Thus, sluggishness becomes the jam for the large-scale hydrogen production from water splitting. consequently, developing efficient OER/HER catalyst is the heart for hydrogen centered new technologies [18]. It is generally known that various TMNs catalysts have been extensively researched as OER electro catalysts for a number of reasons, chief among them being their abundance on Earth, high catalytic activity, and excellent chemical stability [19,20]. Among these nickel-based catalysts are potential electrocatalyst and have showed high oxygen catalytic activity towards OER [21]. However, because of their poor electrical conductivity and unavailability of oxygen adsorption sites, Ni-based catalysts currently have less effective OER activity.

Several attempts have been made to address these inherent flaws with nickel based catalysts [22]. The dissociation of O-O bonds and the release of OH products during the OER process remain the bottleneck issues for Ni-based catalysts, despite advances in research. It is well known that its strong oxo-group affinity can be changed toward high oxygen-relative catalytic activity due to interfacial electron interaction between hetero valence metal atoms at the hetero structure interface [22]. It is thought that by creating a hetero structure out of semi-conductive nickel oxides and metallic nickel nitrides, the oxo-group affinity of Ni sites within a Ni-based catalyst can be effectively controlled [13].

2. 2 Theoretical Background of Electrocatalytic Kinetic Parameters

2.2.1 Overpotential

Overpotential (η) is one of the most crucial criteria used to assess how well target electrocatalysts work. The ideal situation would be for the applied potential to match the

reaction's potential at equilibrium while driving a particular reaction. But in practice, to get over the electrode kinetic reaction barrier. According to the Butler-Volmer equation at high anodic overpotential circumstances, the anodic end is primarily responsible for the total current, with the cathodic end having little to no influence. As a result, the Butler-Volmer equation can be expressed more simply represents as path, the electron transfer rate is typically not the limiting factor at greater current densities; instead, restrictions result from bringing reactants to the electrochemical reaction surface or transferring products to the bulk solution. The rate at which the electrode potential changes with current when the current is low is known as the charger (electron) transfer overpotential and is correlated with the limiting rate of electron transfer across the electrode-solution interface. It is crucial to specify the current density of the reported overpotential since different current densities will correspond to different overpotential values [23,24].

$$E = E^{0\prime} + \frac{RT}{nF} + ln\frac{C_o}{C_R} \tag{2.2}$$

$$\eta = E\text{-}E_{eq} \tag{2.3}$$

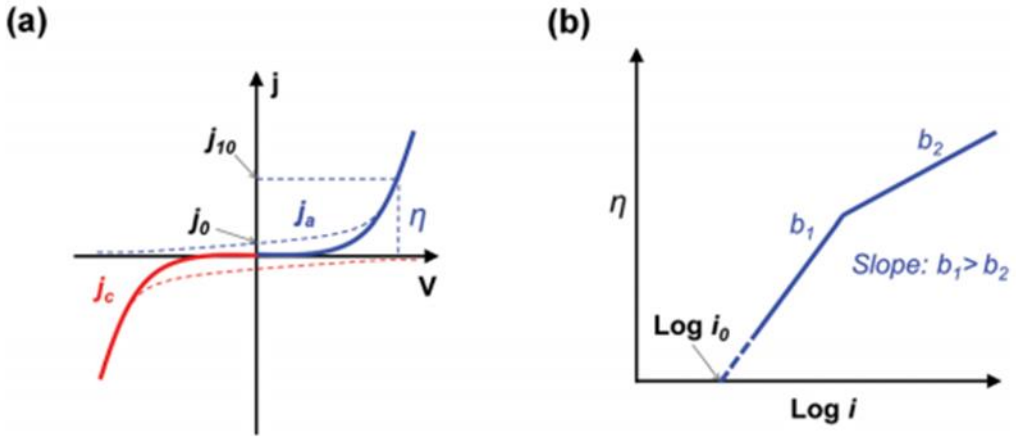

Figure 2. 1 shows the polarization curves for the anode (blue) and cathode (red) electrodes. When ja = -jc, (j0) is the exchange current. For one to report overpotential (η) at this present (assume the area is 1 cm2) value, j10 is a generally accepted number. (b) The exchange current density (i0) in the vs. log i curve might be determined by projecting the curve to = 0. The Tafel slope is slope b, and it is usually believed that the greater the slope, the inferior the electrode

kinetics will be, with slower current increasing at the similar potential as in the case of (b1 and b2).

2.2.2 Tafel equation and Tafel slope (b).

In order to have a substantial magnitude of current density (i), it is necessary to apply a high overpotential (ɳ) practically. Generally speaking, a smaller overpotential (ɳ) is preferred together with a quicker rise in the corresponding current density (i). Application and the current density (i). Equation (2.4) of the well-known Butler Volmer model can be used to describe overpotential [1].

$$i = io[\exp\left(\frac{\alpha_a \, nFE}{RT}\right) + \exp\frac{\alpha_a \, nFE}{RT}] \tag{2.4}$$

According to the Butler-Volmer equation and Figure 1(a), at high anodic overpotential circumstances, the anodic end is primarily responsible for the total current, with the cathodic end having little to no influence. As a result, the Butler-Volmer equation can be expressed more simply as eqn (2.5), also referred to as the Tafel equation.

$$i = io\exp\frac{\alpha_a \, nFn}{RT} \tag{2.5}$$

In order to compute the density of exchange current (i0) and Tafel slope (b), eqn (2.6) might be rewritten as eqn (2.10) by converting the Tafel equation to logarithm function form. The Tafel slope (b) could be described by the equation (2.11), so from this one can deduce that the Tafel slope (b) is defined as the rate at which the current rises relative to the overpotential (), and that the transfer coefficient () has a significant influence on its value [25].

$$\log(i) = \log(i_o) + \frac{\eta}{b} \tag{2.6}$$

$$b = \frac{\partial \eta}{\partial \log(i)} = \frac{2.303\mathrm{RT}}{\alpha F} \tag{2.7}$$

A smaller Tafel slope (b), as shown in Figure 2(b), suggests that current density can increase more quickly with a smaller overpotential (ɳ) shift (i.e., a quicker reaction rate constant), which implies good electrocatalytic kinetics. In addition, Tafel slope (b) offers useful and informative details about the reaction's mechanism, particularly for clarifying the step that determines rate. This can

be quite beneficial for comprehending the basic interactions between the electrocatalyst and the reactant [26].

2.2.3 Plausible paths of Oxygen Evolution Reaction (OER)

Equation (2.8) draws in the first half reaction in water splitting of OER. It should be noted that the cathode and anode components of the water splitting reaction behave differently in acidic (eqn (2.9) and (2.10)) and alkaline (eqn (2.15) and (2.16)) scenarios. Many researches have hypothesized plausible processes for OER at the anode electrode in either acid (eqn (2.11)- (2.15)) or alkaline instances (eqn (2.18)- (2.22)), and there are some differences and similarities among these plausible mechanisms. Despite the fact that the reaction that creates oxygen is likely the main point of difference, the same intermediates, such as MOH and MO, are used in the majority of the hypothesized pathways. Figure 2 shows that two distinct methods have been observed for generating oxygen from a MO intermediate. The green path is the one shown in Figure 2 by the direct combining of 2MO to generate O_2 (g) (eqn (2.13)), as well as its participation in the formation of the MOOH intermediate (eqn (2.14) and (2.21)) which thereafter decomposes to O_2 (g) (black route in Figure 2; (eqn (2.15) and (2.22)). Despite these differences, the formatted bonding (M-O) within the intermediates (MOH, MO, and MOOH) are crucial for the full electro catalytic capacity in the electrocatalysis of OER, which is usually accepted to be a heterogeneous reaction.

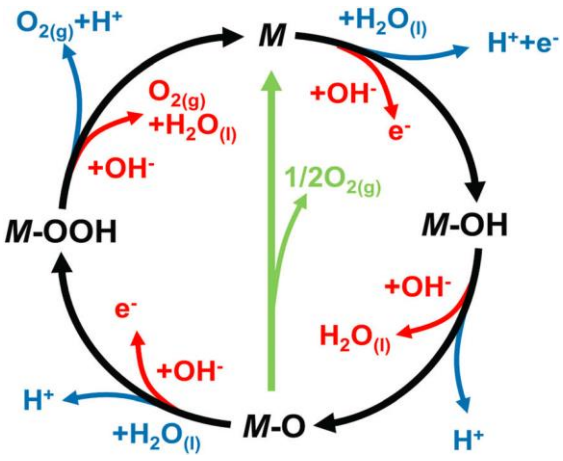

Figure 2. 2 The OER mechanism for acid (blue line) and alkaline (red line) Conditions shows that the OER entails the creation of a peroxide (M-OOH) intermediate (black line), though there is also

a possibility of producing oxygen directly through the reaction of two nearby oxo (M-O) intermediates (green line).

2.2.4 Oxygen Evolution Reaction Mechanism under Acidic Conditions

There are some differences and resemblances among the many hypothesized processes for the OER at the anode electrode for either acidic (eqn (2.11)- (2.15)) or alkaline circumstances (eqn (2.16)- (2.22)) conditions that have been put forth by various research groups. The majority of the hypothesized methods use the similar intermediates, like MOH and MO, but the main distinction is possibly centered on the process that creates oxygen [21,24].

$2H_2O \rightarrow 2H_2 + O_2$ (2.8)

Cathode reaction:

$4H^+ + 4e \rightarrow 2H2$ E_0 c = 0 V (2.9)

Anode reaction:

$2H_2O$ (l) $\rightarrow O_2$ (g) + $4H^+$ + 4e-E_0 a = 1.23 V (2.10)

Proposed mechanism under acidic conditions

$M + H_2O$ (l) $\rightarrow$MOH + H^+ + e- (2.11)

MOH + OH$\rightarrow$MO + H_2O (l) + e- (2.12)

$2MO \rightarrow 2M + O_2(g)$ (2.13)

MO + H_2O (l) $\rightarrow$ MOOH + H^+ + e (2.14)

MOOH + H_2O (l) $\rightarrow$ M + O_2 (g) + H^+ + e^- (2.15)

2.2.5 Oxygen Evolution Reaction Mechanism under Alkaline Conditions

The HER and OER reactions take place on the cathode and the anode, respectively, in a standard electrochemical water splitting ($2H_2O$ $2H_2 + O_2$)[24].

In alkaline conditions HER follows the reaction pathway of

Cathode reaction:

4H2O+4e$\rightarrow 2H_2$+ $4OH^-$ E_0 c = 0.83 V (2.16)

while OER follows Anode reaction**:**

$4OH^- \rightarrow 2H_2 + 2H_2O(l) + 4e$ E0 a = 0.40 V (2.17)

Electrolysis becomes more complicated in OER due to the four-electron transfer process, which also causes a significant energy loss. MO-, 2MOH-, and MOOH type intermediates (where M is the surface metal cation) are frequently produced during the electron transfer process within OER and are essential for the overall electrocatalytic activity. We propose the likely mechanism for

$M + OH^- \rightarrow MOH$ (2.18)

$MOH + OH^- \rightarrow MO + H_2O + e$ (2.19)

$2MO \rightarrow 2M + O_2$ (2.10)

$MO + OH^- \rightarrow MOOH + e$- (2.21)

$MOOH + OH^- \rightarrow M + O_2 + H_2O + e$- (2.22)

OER at the anode in an alkaline environment

2.2.6 Mechanism of Hydrogen Evolution Reaction in Alkaline Solution

The straightforward steps of HER in basic media are as follows:

Total: $2H_2O + 2e^- \rightarrow H_2 + 2OH^-$ (2.23)

Volmer Step: $M + H_2O + e^- \rightarrow M - H^p + OH^-$ (2.24)

Heyrovsky step: $M - H^p + H_2O + e^- \rightarrow H_2 + M + OH^-$ (2.25)

Tafel step: $2M - H^p \rightarrow H_2 + 2M$ (2.26)

M-H* is the hydrogen adsorption on the active site above the catalyst, and M is the catalyst's active site. The Volmer, Heyrovsky, and Tafel stages are a part of the HER procedure. Water is dissociated to create a reactive Had intermediate in the Volmer phase. Another H_2O is adsorbed to M-H* in the Heyrovsky step, where it interacts with the second electron to produce H_2 and OH. Two neighboring M-H* combine in the Tafel stage to produce H_2. Two pathways—Volmer-Tafel or Volmer-Heyrovsky reactions [27] consisting of three sequential stages—water dissociation, water adsorption, and hydrogen production—will be followed by an entire HER process.

2.2.7 Stability of Electrocatalysts

Apart from catalytic activity, electrocatalyst operating stability is another issue to consider when evaluating them for practical applications. Using potentiodynamic or Chronoamperometry techniques for measuring the change in voltage with time, or chronopotentiometry to detect the change in current over time, stability may typically be determined in several hours of measurement. The activity curve is then used to determine the level of stability. To improve stability even further, it's vital to first comprehend the chemical and physical activities that take place on the catalyst surface during reactions [28,29]

2.3 Historical Background of Nickel Nitride Electrocatalyst

Water splitting is one of the most important electrochemical processes for hydrogen production, demanded by the need for clean energy sources. Hydrogen is a clean fuel that can contribute significantly to overcoming climate change and to the reduction of fossil fuel consumption. In this sense, the investigation of effective and inexpensive catalysts able to drive the reaction of water splitting has become a general field of research in electrocatalysis. It involves the dissociation of water its constituent elements being hydrogen and oxygen through various energy inputs. We can use the produced hydrogen as a clean fuel, thereby reducing greenhouse gas emissions and ensuring energy supply security [30,31].

2.3.1 Initial recognition of transition metals

Due to their unique features and possible applications, TMNs have become a research interest of various scientists. First-principles density functional theory research studied their structural, electrical, and magnetic characteristics in the recent past. [32]. usually display outstanding stability, hardness, and conductivity, making them vital for technological applications [33]. Lattice constant and stability change down the periodic table. Group IVB nitrides were found to be more stable than the Group VIB ones, according to [32]. From the TMNs, ScN, YN, and LaN are semiconductors with indirect band gaps and may offer tremendous potential for device applications, according to [33].The early TMNs were examined for their oxidation, which revealed that the initial adsorption and dissociation of O_2 are exothermic and that ScN is different from

other TMNs like TiN and VN [34]. Magnetic characteristics have also been reported with various TMNs, in particular for the M_4N phases[35].

With high surface reactivity toward electrocatalytic reactions, TMNs have emerged as one of the most prospective alternatives to noble-metal-based electrocatalysts in energy conversion applications[36]. Actually, TMNs exhibit similar surfaces and electronic structures with precious metals for the prosperity of various electrocatalytic reactions involved in hydrogen evolution, oxygen evolution, and oxygen reduction [37]. Embedding nitrogen atoms in a metal lattice can reinforce increased electron density and change the d-band center's catalytic activity. Therefore, nanostructured TMNs have improvements in performance because of higher dispersion and more exposed active sites[38]. Recent efforts have gone into the preparation of monometallic and Mult metallic TMNs, while much effort has been devoted to optimizing their electrocatalytic properties by exploring various synthetic methods [36]. Although quite a number of developments have been made recently, poor preparation methods and enhancements of performance are still at the frontiers of development challenges with TMN-based catalysts [37].

2.3.2 Development of electrocatalyst

A. Nickel- Based Oxides OER Electrocatalysts and their Activities

When compared to the metallic state of the Ni, Fe, Co, and Mo elements in NiFe alloys, the spinel-type $NiMO_4$ oxide[23] frequently exhibits +2 and +3, +5 respectively oxidation states, which are much closer to OER region oxidation states. However, because of their amorphous kind, Ni-based oxides catalysts decompose gradually over time [39].

As a result, crystallinity balance is critical for OER to achieve high durability with rigid structures. Large electrochemical active surface area (ECSA) amorphousness, on the other hand, is critical for the development of highly developed Ni-based OER electrocatalysts with high activity. Pristine $NiCo_2O_4$ and support-based $NiCo_2O_4$[40], as well as $NiMoO_4$ [41–43], exhibit a similar trend.

Table 2. 1 Ni-based oxides OER electrocatalysts samples (modified Ayesha K.et al. 2019)

Catalyst	KOH Electrolyte [M]	Onset potential [V]	Specific current density	Overpotential [mV]	References

			[mAcm^{-2}]		
$NiFe_2O_4$NP	0.1	1.67	10	440	[44]
$NiFe_2O_4$NP	0.1	1.70	10	470	[44]
$Ni_{0.5}Fe_{2.5}O_4$	1	-----	20	540	[45]
$NiFe_2O_4$	1	---	20	530	[45]
$Fe_{40}Ni_{60}O_X$	0.1	1.41	0.5	230	[46]
$Co_{40}Fe_2O_4$	0.1	1.41	0.5	270	[46]

B. Nickel- Based Layered Double Hydroxide Nanosheets OER Electrocatalysts

Layered double hydroxide (LDH) is a 2D ionic material division made up of positively charged mono, di, and trivalent metal cations and counterpart anions with solvent molecules in the interlayers [47]. Cations (e.g. Li+, Ni^{2+}, Mg^{2+}, Ca^{2+}, Mn^{2+}, Co^{2+}, Cu^{2+}, Zn^{2+} and e.g. Al^{3+}, Co^{3+}, Fe^{3+}, Cr^{3+} and [48]. The intercalated anions are typical carbonates (CO_3^{-2}), although other anions (such NO^{3-} , SO_4^{2-} or Cl^-) can easily replace them. Since the LDHs is adjacent to an electrolyte with anion exchange, it has become more attractive for electrochemical reactions. Although the main drawback associated with Ni-based LDH is its low conductivity (Ni_3Fe LDHs = 1.943 S/cm, Ni_3Fe LDHs-NH_3 = 3.759 S/cm, Ni_3Fe LDHs-Ar = 3.061 S/cm), a challenge with hydroxides [49]. This barrier can be overcome by growing LDH directly on conductive substrates such carbon nanotubes, graphene, as carbon cloth, Ni foam substrate, carbon quantum dots, and other substrate materials, or by hybridizing with conductive materials [50–52] . Table 2 lists some Ni-based LDH OER electrocatalysts that have been reported to have OER activity.

Table 2. 2 shows samples of Ni-based LDH OER electrocatalysts.

Catalysts	Electrolytes [KOH]	Overpotential (mV) at Specific current density (mAcm^{-2})	references
NiOOH	0.1M	375 @ 5	[53]
NiFe-LDH	1 M	300 @ 10	[54]

NiCo-LDH	1 M	335 >>	[54]
NiCr-DH	0.1M	310 at 1	[55]
NiMn-DH	0.1M	380 >>	[55]
NiFe-DH	0.1M	270 >>	[55]
NiCo-DH	0.1M	500 >>	[55]
$Ni(OH)_2$	0.1M KOH	410 >>	[55]
NiCu-DH	0.1M KOH	450 >>	[55]
NiZn-DH	0.1M KOH	>500 >>	[55]

C. Nickel-Based OER Electrocatalysts Lacking Support

Without the aid of any support, Kun Xu et al. [41] produced enhanced a Ni_3N nanosheets OER catalyst, which is a 2D material smaller than 3 nm. Ni_3N nanosheets have stronger OER activity with a Tafel slope of 45 mVdec-1 than massive Ni_3N and NiO nanosheets (85 mVdec-1 and 59 mVdec-1 respectively). This is due to the increased metallic conductivity and faulty crystal. This Tafel slope is lowered, allowing Ni_3N nanosheets grown on carbon fabric to potentially reach 52.3 mA/cm^2 density of current with only 250 mV of overpotential. In addition to a new method for making effective conducting OER electrocatalysts, this work places more emphasis on 2D metallic materials in the realm of energy conversion and storage.

D. Nickel-Iron/Cobalt/Manganese Nitrides OER Electrocatalysts

Without the use of any support material, Guo, H. P. et al. [42] produced extreme thin holey 2D-nickel-based cobalt/manganese/iron nitride nanosheets that were less than 1 nm thick by ammonolyzing the necessary hydroxide precursors. Due to the excessive lattice spacing and crystalline structural design with good orientation, actively catalytic sites are abundantly exposed and come from both the area close to the boundaries of formed holes and from excess exposed surfaces, making them suitable for the transportation of transitional reaction products and the diffusion of produced gases.

As OER electrocatalysts, these metallic nitride holey nanosheets exhibit electrocatalytic properties. For 2D holey Ni_3Fe nitride nano sheets to produce the approximately 100 $A.g^{-1}$ A

current density with a very low overpotential (300 mV), they must be less in size than 2D holey Ni_3Co nitride nano sheets (340 mV), 2D holey Ni_3Mn nitride nano sheets (429 mV), and IrO_2 (465 mV). In contrast to commercial IrO_2, the 2D holey Ni_3Fe nitride nanosheets exhibit a significant improvement toward OER with a 25 times higher activity to supply 100 Ag current density. The increased ECSA and good intrinsic electrocatalytic properties of the 2D- Ni_3Fe nitride nanosheets are largely responsible for their robust electrocatalytic activity. Additionally, the addition of nitrogen significantly increased the lattice gap, resulting in more electrochemically accessible interior layer.

E. Nickel-Based OER Electrocatalysts with Support

Shalom, M. *et al.*,[56] synthesized 3D-Ni_3N on Ni-foam support which exhibits low overpotential customized foamshows enhanced OER activity. The formation of NiOOH is necessary to increase the OER that occurred at elevatedpotentials (E >1.53 V). In Ni_3N /Ni-foam NiOOH oxidation peak intensity maxima after 500 CV cycles, does not change.The NiOOH peak formation intensity shows increased active Ni amount on the surfaces. Enhancement in activity can beattributed to $Ni(OH)_2$ layer on nitride surface (Ni_3N /$Ni(OH)_2$) with improved lattice matching. Consequently, in lower overpotentials for H_2O splitting on NiOOH surface. The 3D- Ni_3N nanosheets grown on Ni-foam displays lesser onset potential (1.55V) in comparison to Ni_3N (1.64 V) bulk and NiO nano sheets (1.65 V) with small Tafel slope 45mV/dec compared tobulk Ni_3N (85mV/dec) and NiO nanosheets (59mV/dec).

F. Nickel-Iron Nitrides OER Electrocatalysts

When employing a method mediated by galvanic replacement, Xu Chen et al [44] demonstrated that 1D- Fe_2Ni_2N support on carbon nanotubes (CNTs) roles as an OER catalyst. Due to the intimate contact that was created, transfer charge on the surface catalyst was improved. First-principal calculations show that Fe_2Ni_2N is metallic and that electron donation is largely provided by Fe atoms, which are located at the corners of crystal formations. The outstanding OER activity was made possible by the synergistic interaction of the metallic 1D- Fe_2Ni_2N activity and conductive CNTs, as verified in coupled with excellent long-term stability (10 $mAcm^{-2}$ = 282 mV overpotential and 38 mV dec^{-1} Tafel slope). When compared to metal/oxide/hydroxide on CNTs and Fe_2Ni_2N alone, in-situ development of Fe_2Ni_2N on CNTs exhibits higher activity in the OER potential range. According to Chen, Q. et al [47] ,. 3D-Ni_3FeN nanoparticles grown on carbon

cloth (Ni_3FeN /CC) produce flexible OER electrocatalysts with Tafel slopes of 59 mV/dec in alkaline (1 M KOH) solution at 241 mV at 10 $mAcm^{-2}$.

Ni_3FeN 3D-sheets were created by Wang et al. [57] and their OER electrocatalysts, grown on Ni-foam support, were shown to be effective and stable. The precursor of Ni_3Fe LDHs is converted into Ni_3FeN through ammonolysis in a widely utilized synthetic technique. Ni_3FeN is made up of nanosheet structures linked together by nanoparticles. There are more active sites for OER in porous sheets nanoparticles stacked electrocatalysts. In comparison to Ni_3Fe LDHs-Ar (250 mV) and Ni-foam NH_3, the Ni_3FeN exhibits a 223 mV overpotential at 10 $mAcm^{-2}$ in alkaline solution (1 M KOH) (330 mV). While the current density is 50 $mAcm^{-2}$, the over potentials of Ni-foam NH_3, Ni_3Fe LDHs, Ni_3Fe LDHs-Ar and Ni_3FeN are 421 mV, 279 mV, 293 mV and 248 mV correspondingly. Likewise, at a current density of 10 $mAcm^{-2}$, the over potential of 3D- Ni_3FeN is close to RhO_2 for oxidation H_2O. Because of its relatively low Tafel slope (223 $mVdecade^{-1}$) among these catalysts, 3D- Ni_3FeN exhibits considerable OER performance. This success deed originates from an intrinsic material property with unique 3D- morphology. Z. Liu et al.,[58] demonstrated the synthesis of 3D- Ni_3FeN on carbon cloth Ni_3FeN /CC) supported by ammonolysis as a hierarchical electrocatalyst in a related report. This catalyst demonstrates improved electrochemical properties for OER in the form of overpotential (105 mV) at 10 $mAcm^{-2}$ with excellent stability. Comparing Ni_3N/CC (340 mV), Fe_2N/CC (400 mV), and RuO_2 to Ni_3FeN/CC over potential, it is found that Ni_3FeN /CC performs better for OER (364 mV). The Ni_3FeN /CC Tafel slope (72 mV dec^{-1}) is small, comparatively to Ni_3N/CC (112 mV dec^{-1}), Fe_2N/CC (128 mV dec^{-1}) and RuO_2 (94 mV dec^{-1}), very rapid charge relocation. Gu, Y., et al.,[59] grew nano size Ni_3FeN particles (NPs) on rGO (reduced graphene oxide) support using a simple aerogels method and for nitration followed by ammonolysis with particle sizes ranging from 35.4 nm to 35.4 nm. Tafel plots generated by LSV were used to estimate the 3D- Ni_3FeN /rGO OER kinetics. Ni_3FeN /rGO has the smallest Tafel slope (54 mVdec-1) when compared to Ni_3Fe/rGO (57 mV dec^{-1}), Ni_3N/rGO (65 mV dec^{-1}), Fe_2N/rGO (93 $mVdec^{-1}$) and Ni_3FeN /rGO (93 $mVdec^{-1}$) (116 $mVdec^{-1}$). The metallic nitride NPs supported on rGO aerogel displayed minor resistance for charge transfer in comparison to Ni_3FeN NPs.

G. Nickel- Cobalt Nitrides OER Electrocatalysts

The hydrothermal method was successfully applied by Lei Han et al., [48] to create 1D-NiCoN porous nanowires supported on carbon fabric before nitration with ammonia. NiCoN porous nanowires have good OER electrochemical performance in 1M NaOH solution, as shown by the OER study, with a small over potential of 0.360 mV at 10 $mAcm^{-2}$ current density, a low Tafel slope of 46.9 $mVdec^{-1}$, and good electrochemical stability. The higher conductivity brought on by the nitrogen content and the intimate contact between the carbon cloth support and the NiCoN catalysts are a few examples of particular morphological characteristics that contribute to the better electrocatalytic performance in 1M NaOH. OER for the half-cell water splitting reaction, nanowire nickel cobalt nitride electrocatalysts showed good stability.

Y. Wang et al.,[60] created Ni-based ternary nitrides 3D-$NiCo_2N$ by growing them on nickel foam (NF) supports and then ammonolyzing them under ammonia flow. Besides that, the creation of 3D interconnected microporous NF with a sizable surface area exposed additional active sites, speeding up (H_2) charge transfer and diffusion. Nickel cobalt nitride electrodes that have already been created exhibit exceptional activity with a 290 mV overpotential for OER to reach a 10mA cm^{-2} current density. LSV of $NiCo_2N$-NF for OER displays at ~1.49 V low onset potential than NF (1.57 V), $NiCo_2O_4$-NF (1.54 V), Co_3O_4-NF (1.53 V) and CoN-NF (1.51 V. Furthermore, the overpotential required to generate a standard current density (i.e. 10 mA cm^{-2}) is 0.29 V. It is less than NF (0.36 V), $NiCo_3O_4$-NF (0.34 V), Co_3O_4-NF (0.32 V), and CoN-NF (0.30 V). The electrochemical stability of $NiCo_2N$-NF OER was evaluated separately at two fixed current densities of 10 and 50 mA cm^{-2}. Since only 0.39 V overpotential is needed to achieve extremely high current density, these TMNs have the potential to be non-noble electrocatalyst for wide-range H_2O electrolysis devices at (300 mA cm^{-2}).

H. Nickel Molybdenum Nitrides OER Electrocatalysts

In order to produce bimetallic 1D-NiMoN nanofibers (NF) at three different temperatures, namely 600, 700, and 800 °C, Bin Chang et al. [50] used a solvothermal approach followed by ammonolysis, the NiMoN-NF700 (synthesized at 700 °C) LSV surpasses the NiMoN-NF500 (410 mV at 50 $mA.cm^{-2}$), NiMoN-NF600 (370 mV at 50 $mA.cm^{-2}$), NiMoN-NF800 (360 mV at 50 $mA.cm^{-2}$) and $NiMoO_4$ nanowires (510 mV at 10 mA). Additionally, RuO_2, NiMoN nanotubes, NiMoP nanowires, NiFeOx film, and NiCo LHD are comparable to the previously described OER

catalysts, as are NiMoN-NF700 nanowires/nanofibers at 296 mV at 10 $mA.cm^{-2}$, 320 mV at 20 $mA.cm^{-2}$, and 367 mV at 10 $mA.cm^{-2}$.

In the first step, NiMO nanorods grown hydrothermally on Ni-foam support were used to create 3D-Ni0.2Mo0.8N OER electrocatalyst, and in the second phase, nitration was used to create Ni-foam@Ni-Ni0.2Mo0.8N. In an oxygen-saturated alkaline (1M KOH) solution, Ni- foam@Ni-Ni 0.2Mo 0.8N OER performance calculations show that this material has a lower overpotential (218 mV) than Ni- foam@Ni4Mo/MoO_2, Ni- foam@$NiMoO_4$, Ni- foam@Ni_3N, and Ni- foam (405 mV). It provides a greater current density than the industrial standard OER electro catalyst RuO2) supported on Ni foam (245 mV). Remarkably, Ni-foam@Ni-Ni 0.2Mo0.8N has a Tafel slope of 55 $mV.dec^{-1}$, which was also smaller than that of Ni- foam @Ni_4Mo/MoO_2 (181 mV dec^{-1}), Ni-foam @$NiMoO_4$ (133 mV $dec^{-1)}$, Ni-foam @Ni_3N (81 mV dec^{-1}), Ni-foam (110 mV dec^{-1}) and even the champion material - RuO_2 on Ni-foam (66 mV dec^{-1}).

Table 2. 3 Lists of Ni-based transition metal nitrides with 1D, 2D, and 3D nanostrucutres nanostructures as OER electrocatalysts.

All these reports have done on 1MKOH electrolyte solution ((modified Ayesha. K et al. 2019.)

Electrocatalysts	Morphology	η(mV)	Over Potential (V vs RHE)	Stability	references
Ni_3N	2D-sheet	1.55	250	Excellent	[61]
Ni_3N/CC	3D-sheet	1.36	190	Good	[58]
Ni_3N/NF	3D-foams	1.39	50	Excellent	[56]
Fe_2Ni_2N/NCT	1D-tubes	1.47	282	Good	[62]
Ni_3FeN	2D-sheet	1.35	300	Excellent	[63]
Ni_3FeN/NW	3D-sheet	1.34	200	Excellent	[57]
Ni_3FeN/CC	3D-sheet	1.33	105	Excellent	[58]
Ni_3FeN/rGO	3D-sheet	1.42	280	Good	[64]
NiCoN/NW	1D-nanofibers	1.53	360	Good	[65]
Ni_3CoN	2D-sheet	1.52	340	Excellent	[63]
Ni_3Co_2N	3D-sheet	1.53	180	Good	[60]

Ni_3MnN	2D-sheet	1.60	320	Excellent	[63]
NiMoN/CF	1D nanofibers	1.32	210	Good	[66]
NiMoN/NF	3D-foams	1.35	218	Excellent	[67]

CNT stands for carbon nanotube, NF stands for nickel foam, NPS stands for nano porous structure, NW stands for nanowires, and OP stands for Onset Potential. TS = Tafel slope = Overpotential, NSP = stacked porous nanoparticles, CC = carbon cloth, CF = carbon fibers,

In conclusion, particular emphasis on nickel-based substances, nickel-based nitrides often exceed their corresponding oxides in terms of stability and performance. Layered double hydroxides, which are also developing contenders, have lower kinetics than nitrides due to their low electrical conductivity (Ni_3Fe LDHs = 1.943 S/cm, Ni_3Fe LDHs-NH3 = 3.759 S/cm, Ni_3Fe LDHs-Ar = 3.061 S/cm). Ni-based nitride electrocatalysts have been developed in a variety of morphologies, spanning from 0D to 3D, and with and without support materials.

In the OER reaction, D-supported (support material such as carbon cloth, Ni-foam, rGO, etc.) electrocatalysts show good stability and activity. Because of their highly orientated crystal structure, Ni-based 3D-architecture OER electrocatalysts with support (i.e. foam support) do not only accelerate electron transfer; instead, they assist the diffusion of intermediate and end products during reactions. Manufacturing TMNs with a specified structure and crystal planes, on the other hand, typically necessitates numerous steps and high temperatures (for TMNs, 800°C); this makes the synthesis expensive, time-consuming, and uneconomical. This is particularly difficult in template synthesis.

When compared to 3D-support electrocatalysts, 2D Ni-based nitride sheet materials with no support often perform better. Ni-metal-based 2D-sheet materials are excellent alternatives for support-free OER electrocatalysts and are gaining prominence and attention. Notable results include 2D- Ni_3N nanosheets, which are known to improve contact with the electrode and consequently electron transport inside the material. The planar sheet layout also adds disordered structure and more active sites for OER. Finally, OER electrocatalysts based on earth plentiful metals and with morphological confinement (e.g. 2D-Ni based nanosheets material) is a budding area of research that holds the promise of developing materials that outperform IrO_2 and RuO_2 electrocatalysts [42].

I. Transition metal nitrides for HER in alkaline solution

The HER performance of transition metal nitrides (TMNs) has shown promise in recent years. TMNs are gradually finding their way into energy gadgets. For example, in AEMFCS, the prepared electrolyzer requires only 1.644 V to reach a big current of 1A, and the prepared Co-N-C catalyst achieves a maximum power density of 275 and 361mW cm^2[56]. The reason that TMNs have such great potential is that N can increase the d-electron density, causing the d-band of TMNs to contract. Because of this one-of-a-kind structure, TMNs will have an electronic structure akin to PGM metals like Pd and Pt. Furthermore, TMNs are high-performance due to their good conductivity and corrosion resistance. Ni_3N and Co_4N, two TMNs, were synthesized by Shalom et al. and Chen et al. TMNs are high-performing due to their resistivity. Shalom et al. and Chen et al. synthesized Ni_3N and Co_4N among other TMNs in 2015[43,57]. As a result, considerable work has been expended in improving the catalytic activity of TMNs toward HER electrocatalysts. TMNs are high-performing due to their resistivity. Shalom et al. and Chen et al. synthesized Ni_3N and Co_4N among other TMNs.

To improve the stability of various TMN catalysts, several design strategies were applied. For example, by making TMNs come into intimate contact with MXene and generating a strong interface junction, high structural stability was achieved. The oxidation of Co_4N through a carbon shell was also greatly suppressed, which increased the stability. As a result, although some design solutions can improve catalytic performance, others can improve TMN stability [58]. The methodologies for rational design of TMN electrocatalysts are classified in a table.4

Table 2. 4 outstanding TMN-based electrocatalysts in 1.0MKOH electrolyte solution (modified Siyaun et al.,2022)

Catalyst	HER			
	η_{10} (mV)	η_{100} (mV)	Tafel slope (mV/dec)	References
Ni_3N/NF	121	254	-	[68]
$FeNi_3N$	75	210	98	[69]
Ni_3NCeO_2/TM	80		122	[70]

Cr-Ni_3N/Ni	37	110	47	[71]
Ni_3N-VN	64	218	37	[72]
Ni_3N-V_2O_3	57	-	50	[73]
NiMoN	110	161	95	[74]
NiMoN/Ni_3N	28	93	49	[75]

2.3 Emergence of Nickel Nitride as Electrocatalyst for Hydrogen Production

In fact, nickel nitride, Ni_3N, is among the latest promising electrocatalysts for hydrogen evolution reactions in water splitting, and its unique metal property and excellent conductivity point toward its broad application in energy storage and conversion systems [76]. It shows an extremely low overpotential of ~50 mV with a high current density for HER in alkaline solutions due to the formation of a $Ni(OH)_2$ layer on the nitride surface[77]. Incorporation of nitrogen vacancies in Ni_3N 1-x significantly improves its HER activity in comparison with its stoichiometric counterpart, Ni_3N, and even outperforms the commercial Pt/C catalysts[78]. Various synthesis methods have been developed to fabricate Ni_3N-based electrocatalysts, including plasma-enhanced nitridation [79]. Even with the promising performance, optimisation of morphology and electronic structure in Ni_3N for full utilization of the electrochemical active site for further improvement of catalytic efficiency in energy-related applications is a challenge[76].

2.3.1 Catalytic Properties of Ni_3N

A. Oxygen Evolution Reaction

Recently, nickel nitride has gradually been considered one of the most promising electrocatalysts of the oxygen evolution reaction in water splitting. Indeed, Ni_3N nanosheets, with their metallic nature and disordered structure, exhibit superior electrical conductivity and increased active sites, which enhance OER activity compared to bulk Ni_3N and NiO nanosheets[61]. Formed $Ni(OH)_2$ on the surface of Ni_3N will contribute to a lower overpotential and easier water

dissociation[77]. Particles of Ni_3N with rich amounts of nickel, in the company of graphitic carbon nitrides, showed excellent OER performance, outperforming the pure Ni_3N and even a benchmark RuO_2 [80]. During the course of the OER, a nanostructured Ni_3N/3N precatalyst underwent self-adaptive surface reconfiguration, forming active NiOOH species responsible for the high catalytic activity [81]. These value-added studies epitomize the excellent electrocatalytic properties of Ni_3N in OER, which have great potential for efficient and cost-effective water splitting.

B. **Hydrogen Evolution Reaction**

Recent research has illustrated that Ni_3N has the best catalytic performance of HER. Further, their catalytic activities have been improved by trying different methods[82]. Yi-Bing Yang et al. in 2024 decreased the energy state of the vacant d orbitals in Ni_3N. They attained an overpotential of 135 mV at 10 mA cm^{-2}. Hu 2024 [83] incorporated vanadium and iron into the Ni_3N nanosheets, which obtained an impressive overpotential as low as 69 mV at 10 mA cm^{-2}. Paquin *et al.,* [35] prepared atomically thin Ni_3N nanosheets that reached 100 mA cm^{-2} at an overpotential of 100 mV. Hu 2024 [83] designed a Ni_3N/Ni heterostructure that needs an overpotential of 144 mV to yield 10 mA cm^{-2}. These studies highlight the possibility of using Ni_3N-based catalysts for HER by demonstrating their high activity and stability with low cost compared to precious metal catalysts.

Nickel nitride (Ni_3N) has garnered significant attention as an effective electrocatalyst for the hydrogen evolution reaction (HER) and other electrochemical processes. Its unique properties, including high catalytic activity, stability, and low cost, make it a promising alternative to precious metal catalysts. This section explores the catalytic properties of Ni_3N, focusing on its performance in hydrogen production through water splitting.

2.3.2 synthesis of Ni_3N electrocatalyst for OER and HER

The synthesis of Ni_3N has so far achieved outstanding success over the years. Most traditional methods of syntheses involve nitridation processes at high temperatures and face serious safety problems and scaling-up issues. The latest development in this field of research has provided advanced synthesis techniques that are efficient and more environmentally friendly. Due to stability, high catalytic activity, and low cost, Ni_3N is one of the best candidates for the OER and

HER. In order to improve this catalyst, various synthesis methods have been developed up to date by often incorporating it into N-C materials. Some major synthesis techniques developed for Ni_3N electrocatalysts are addressed as follows.

A. Magnetron Sputtering

Magnetron sputtering was able to synthesize Ni_3N directly with nitrogen vacancies, which, in turn, significantly enhances the catalytic properties toward hydrogen evolution[84]. Intrinsic magnetism induced by the same sort of vacancy was previously demonstrated for other nitrides, such as GaN and BN, offering media for long-range magnetic interactions[85]. The synthesis parameters, including reaction time and temperature, would significantly influence the material's stoichiometry and defect structure since it affects not only the magnetic properties but also the electronic properties of the resultant material[86]. The concentration of oxygen partial pressure during deposition in nickel ferrite thin films plays an important role in dictating the saturation magnetization due to the result caused by the vacancy concentration, which in turn influences the electrical conductivity[87]. These studies identified control of vacancy concentrations in nitride materials as one of the methods their magnetic and electronic properties could be tailored for various.

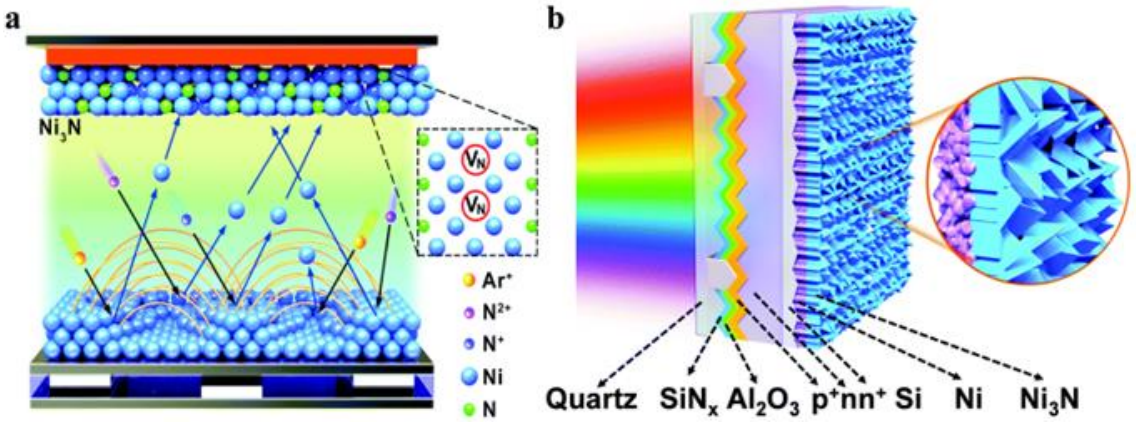

Figure 2. 3 (a) Schematic illustration of sputter-deposition of Ni_3N film with N-vacancies. (b) Schematic illustration of the structure of Si photocathode consisting of a burie 1d-junction Si coated with sputter-deposited Ni_3N/Ni cocatalyst.

The nitrogen species from dissociation and ionization of nitrogen atoms permeate into the Ni lattice, resulting in the formation of Ni_3N with N-vacancies as illustrated in Figure 2.3 a**.** To evaluate

the PEC performance of Ni_3N/Ni films as cocatalyst, Si photocathodes were fabricated with p^+nn^+ buried-junction structure, as illustrated in Figure 2.3 b

The method produces Ni_3N with a high percentage of nitrogen vacancies, which enhances hydrogen binding and catalytic performance. For instance, a study reported a low overpotential of 89 mV at 10 mA cm^{-2} in alkaline media, showcasing its efficiency for HER [84]

B. Electrodeposition

Recent efforts have focused on the preparation and applications of Ni_3N with nitrogen vacancies. Indeed, Ni_3N1-x prepared by plasma-enhanced nitridation of Ni foam exhibits significantly improved hydrogen evolution reaction activity in alkaline conditions, even superior to that of its stoichiometric counterpart of Ni_3N, as reported. Nitrogen vacancies in Ni_3N enhance the adsorption behavior of water molecules and hydrogen adsorption-desorption for better catalytic performance, as also reported by [78]. The Ni_3N with nitrogen vacancies has also been synthesized in hierarchical porous 3D Ni_3N-CoN/NC heterojunction nanosheets, which exhibited excellent performance as a flexible supercapacitor electrode[88]. $Ni_3N0.85$ with engineered nitrogen vacancies in lithium-sulfur batteries accelerates the conversion of polysulfides and accordingly exhibits high discharge capacity and low cycle decay per cycle[89]. These works introduce nitrogen vacancy-containing Ni_3N for energy-related applications and show improved catalytic activities and electrochemical performances.

The process involves depositing nanoparticles of nickel on conducting substrates, such as nickel foam, through subsequent thermal nitridation. Most of these syntheses involve a cathodic electrodeposition in a solution containing nickel salt, followed by ammonia gas at higher temperatures to produce Ni_3N. This method has yielded Ni_3N/Ni interfacial catalysts, which ensured extraordinary HER activity with an overpotential of almost zero, besides robust long-term durability[90]**.**

3.3.3 Performance on Stability and Durability

Long-Term Stability: Whereas current literature has proven the long-term stability of nickel-based catalysts towards different electrochemical reactions, Ni_3N has shown better activity and stability in hydrogen oxidation and evolution reactions in both alkaline media [91]. A Ni-based reference catalyst exhibited fantastic stability over 800 hours in ammonia decomposition with only

1.5% of activity loss[92]. The porous Ni_3N nanosheet arrays showed great durability toward methanol oxidation, retaining 72.58% of their activity after 20 hours[93]. Encapsulation strategies have been developed further for enhancing stability. A hexagonal boron nitride-encapsulated single-crystal Ni23B6 catalyst maintained performance for more than 2000 cycles and 20 continuous hours in acidic media [94]. Considered together, these studies represent a pathway to reach long-term stability with nickel-based catalysts in various electrochemical applications**.**

Temperature control test results using 490 mL min^{-1} NH3 and 10 mL min^{-1} Ar, 500 mg reference catalyst, and a setpoint of534 °C for the three-point controller

Resistance to Degradation: It is shown that nickel-based catalysts are active toward the OER in alkaline media; however, they suffer from degradation. Electrodeposited Ni(OH)2 degrades through a process that involves two steps: first, partial reduction of γ-NiOOH into β-Ni(OH)2 and then transformation into unstable γ-NiOOH [95]. Nickel nitride catalysts exhibit activity and stability in both oxygen reduction and evolution reactions under acidic and alkaline conditions[96]. The ultrathin nickel oxide defect layer formed with Ni-N at the interface thus provides excellent OER performance and durability for the carbon-coated nickel nitride nanostructure[17]. Several strategies have been proposed in view of improving catalyst stability: alloying, nano structuring, and use of high-density carbon substrates. It is further desirable to develop standardized accelerated lifetime tests and universal Figure s of merit on stability by which different catalysts can be compared on equal footing to drive further improvements in the field of OER catalyst research [97]. The work of Spöri et al. (2017).

2.3.4 Active Sites and Mechanistic Insights

A. Active Sites

The presence of nitrogen vacancies and specific surface terminations in Ni_3N enhances its catalytic activity. Lately research has focused on how active sites can enhance the catalytic activity of Ni_3N toward oxygen evolution reactions. In this respect, oxygen vacancy and specific surface termination have proved vital to improving OER performance. [98] demonstrated that the oxygen vacancies in Ni_3N-CeO2/NF heterostructures are offering more active sites, which has resulted in a low overpotential for OER and HER[61]. It has been reported that, compared to bulk Ni_3N, Ni_3N nanosheets with a disordered structure provide more active sites for OER. [22] found that the presence of a strongly coupled NiN-O nanointerface in Ni_3N/NiO composites greatly enhanced OER efficiency. Recent research has focused on how active sites can enhance catalytic activity. In

this regard, [81] has stated that during OER, Ni_3N@/ 3N precatalyst underwent self-adaptive surface reconfiguration and hence formed NiOOH species responsible for the high catalytic activity. These works together suggest that the introduction of engineered active sites, including vacancies, interfaces, and surface structures, plays a very important role in the enhanced OER activity of Ni_3N-based catalysts.

B. Catalytic Mechanisms

The participation of Ni_3N in electrocatalysis has often shown involvement with an underlying mechanism of electron transfer that is relatively complex. In this respect, for the OER to occur, these structural changes will create active Ni-O-Fe bonds to enable rapid electron transport.

DFT studies have demonstrated how varied oxidation states of nickel are in dominance along the reaction coordinates toward the optimization of substrate interactions.

The partial chemical restructuring of the nickel center's is of utmost importance: under operational conditions, it might greatly contribute to stability and activity in the long run. This enables the potential creation of new active sites that are much more effective in catalysis. Advanced characterization techniques of X-ray absorption spectroscopy were carried out in situ to follow these changes, giving insight into how the active site actually evolves during catalytic processes**.**

The mechanism of Ni_3N during electrocatalysis often involves complex electron transfer processes. For instance, during OER, structural transformations lead to the formation of active Ni-O-Fe bonds that facilitate electron transport. Density Functional Theory (DFT) calculations indicate that varying oxidation states of nickel play a significant role in determining reaction pathways, optimizing interactions with substrates. Under operational conditions, nickel centers undergo partial chemical restructuring, which is vital for maintaining stability and activity over time. This restructuring can generate new active sites more effective in catalysis

Advanced characterization techniques, such as X-ray absorption spectroscopy (XAS), have been utilized to monitor these changes in situ, providing insights into how active sites evolve during catalytic processes [99]. Normally, the performance assessment of nickel nitride catalysts is judged from overpotential and current density in the course of electrochemical reactions. Ni_3N indeed shows low overpotentials for hydrogen evolution, thus making it competitive with other active materials.

The interaction of structural features with electronic properties is extremely important, where

modifications like nitrogen doping enhance the electrocatalytic activities by optimizing the binding energies and enhancing the charge transfer[100].

2.4 Nickel Nitride Enclosed by shells for OER and HER

The wrapped shell nickel nitride (Ni_3N) materials has emerged as a promising approach to enhance the efficiency of electrocatalysts for the oxygen evolution reaction (OER) and hydrogen evolution reaction (HER). Recent advancements in this field focus on improving catalytic performance, stability, and scalability through innovative synthesis methods and material design.

2.4.1 Synthesis Techniques

A. One Pot Process Method

Studies have introduced various synthesis methods to effectively integrate Ni_3N with shells. Recent advances in one-pot synthesis have given way to the development of efficient ways to synthesis carbon-based composites, which exhibited improved catalytic performances [101]. Realized a nickel nanoparticle-embedded carbon monolith with hierarchical porosity using the one-pot nano casting method and found it catalytically active for the reduction of 4-nitrophenol. Wen et al., [102] reported a one-pot/one-step synthesis of N-doped graphene/CNT hybrids with superior electrocatalytic performance. The soft templates were used to synthesize the nanoporous carbon nitride solids by [103], further expanding the group of nitrogen-rich carbon materials. Paraknowitsch *et al.*, [104] designed a versatile one-pot sol-gel method using multifunctional surfactants for the preparation of metal-doped mesoporous composites with applications in sustainable catalysis and energy. These references together hereby reveal that one-pot synthesis enables the fabrication of diverse advanced carbon-based material systems featuring tailored properties and higher catalytic activities in an efficient manner.

Research has revealed that the Ni_3N@N-C composites prepared by one-pot processes exhibit very impressive performance metrics. It was reported that such composites could show rather low overpotentials in HER , for example, as low as about 89 mV at 10 mA cm^{-2}, hence competing with noble metal catalysts like platinum. Improved hydrogen adsorption and desorption kinetics owing to the porous structure develop the HER performance**.** Similarly, the performance of OER has been

improved, and such composites have expressed low overpotential due to their optimized structure and electronic properties upon nitrogen doping. The nitrogen functionalities within the carbon matrix play an important role in facilitating better adsorption of the reaction intermediates. The active sites of both HER and OER have been majorly contributed by interactions between nickel atoms in Ni_3N and nitrogen species inside the carbon matrix. Pyridinic nitrogen has shown enhancement in electron transfer rate. DFT studies have shown that at the interface of Ni_3N and N-doped carbon, electronic interactions optimize the charge transfer process in electrocatalytic reactions and further enhance catalytic efficiency.

The method simplifies the synthesis process by making several steps a one-pot process hence saving time and reducing the possibility of contamination by several materials handling. The fact that it employs precursors that are easily available and synthesizes them under mild conditions makes the process economically viable compared to conventional techniques that involve high-temperature nitridation. In Conclusion, the synthesis of nickel nitride encapsulated with nitrogen-doped carbon through a one-pot process is a very effective route to yield an advanced electrocatalyst toward both OER and HER. The development of the technology allows for creating porous structures that mark a leap in the advancement of technology involved with electrocatalysis. Further investigation in optimizing this synthesis technique will further improve performances of Ni_3N@N-C composites in renewable energy systems [105–107].

B. Chemical Vapor Deposition (CVD) Method

CVD techniques have been optimized to produce uniform layers of N-doped carbon over Ni_3N nanoparticles. This method allows for precise control over the nitrogen content and morphology, which are crucial for maximizing catalytic performance

Recent efforts have focused on the development of CVD techniques of equally N-doped carbon over metal nanoparticles for enhanced catalytic activity. Iwasaki et al., [108] came up with a one-step CVD process to synthesize tunable morphology and nitrogen content N-doped carbon nano coils by using nickel-iron catalysts. Wu et al.,[109] pointed out that precursor selection and synthesis chemistry have immense importance in the development of M-N-C catalysts, whereby the incorporation of nitrogen was believed to play a great role in nanostructures for improved ORR activity. Consequently,[110] successfully prepared Fe-doped Ni3C nanodots dispersed in N-doped carbon nanosheets that showed excellent electrocatalytic properties toward both HER and OER.

Li et al., [111] explained that enhanced chemical reactivity is present with metal nanoparticles supported on mesoporous N-doped carbons and carbon nitrides. They added that such enhancement is due to electronic interaction between the metal and semiconductor components, affording improvements in the catalytic performances.

The evidence that such composites can realize low overpotentials for HER, around 89 mV at 10 mA cm^{-2}, may place them in competition with noble metal catalysts such as platinum. The porous structure enhances the hydrogen adsorption and desorption kinetics, hence improving the HER performance. Various composites have enhanced their OER performance by realizing low overpotentials because of the optimized structure and electronic properties due to nitrogen doping. Normally, nitrogen functionalities within the carbon matrix play a crucial role in facilitating better adsorption of reaction intermediates**.** First of all, understanding the mechanism which stands behind the improved performance of Ni_3N@N-C composites synthesized via CVD is of vital importance. The active sites for both HER and OER have been majorly ascribed to the interactions between nickel atoms in Ni_3N and nitrogen species in the carbon matrix. It has been shown that pyridinic nitrogen enhances electron transfer rates. DFT calculations indicate that the electronic interactions at the interface between Ni_3N and N-doped carbon optimize the charge transfer processes during electrocatalytic reactions, leading to further catalytic efficiency enhancement.

In conclusion, among all the ideal methods for the synthesis of nickel nitride enclosed by nitrogen-doped carbon materials, chemical vapor deposition stands out. The CVD is that important in developing electrocatalytic technologies, in that upon allowing the fabrication of porous structures, it increases the catalytic activity toward applications of OER and HER. Further studies of optimization on this synthesis route will result in higher performance improvement in systems of renewable energy using Ni_3N@N-C composites [105,106,112–114].

C. Magnetron Sputtering Method

Magnetron sputtering is a versatile physical vapor deposition technique that has so far been successfully utilized to develop hierarchical nanoarrays of nickel and its nitride, nickel nitride, on conductive substrates. It opens an avenue to integrate these materials with nitrogen-doped carbon, hence enhancing their electrocatalytic performances toward the oxygen evolution reaction and hydrogen evolution reaction.

Several literatures reported that the magnetron sputtering-prepared Ni/Ni_3N nanoarray showed excellent performance metrics of OER and HER. Several performances of overpotential for HER have been compared. In some cases, this overpotential was comparable to the noble metal catalysts. This is due to increased availability of the active sites because of the hierarchical structure, thus improving the mass transport which enhances reaction kinetics. Similarly, OER performances have also been improved with optimized structural characteristics and improved electronic properties upon integration with N-doped carbon. The presence of nitrogen functionalities favors enhanced adsorption of reaction intermediates, hence further improvement in catalytic efficiencies.

The active sites for HER and OER can be ascribed mainly to synergistic effects arising from the interaction of nickel atoms in Ni_3N and nitrogen species residing within the carbon matrix. Pyridinic nitrogen was found to increase the electron transfer rate. DFT studies on the interface of Ni/Ni_3N and N-doped carbon suggest that the electronic interactions between the two will optimize the processes of charge transfer during electrocatalytic reactions, thus further enhancing catalytic efficiency.

In summary magnetron sputtering of hierarchical nanoarrays of nickel and its nitride on conductive substrates is an effective synthesis method. When these are integrated with nitrogen-doped carbon, their corresponding electrocatalytic performance significantly improves for both OER and HER applications. Further optimization of this synthesis technique will lead to further improvement in performance in renewable energy systems. sputtering parameters allows for the potential control of the morphology of deposited Ni and Ni_3N species, thus enabling hierarchical structures with high surface area and improved catalytic activities.

The integration of N-doped carbon can be further performed either after the deposition of Ni or Ni_3N by subsequent CVD processes or pyrolysis of carbon precursors in a nitrogen-rich atmosphere. The thus-obtained composite exhibits superiorities from not only the high conductivity of metals but also the enhanced catalytic property provided by N-doping. [105,106,113,115]

D. Hydrothermal and Solvothermal Methods

Hydrothermal and solvothermal methods are regarded as effective routes to synthesize Ni_3N within nitrogen-doped carbon matrices. Both the approaches utilize the specific characteristics of solvent

in a high-pressure environment to ultimately yield the materials with desirable structural properties, enhancing the catalytic activities toward OER and HER.

Hydrothermal and solvothermal synthesis of Ni_3N@N-C composites have shown fantastic metrics in their performances. Several reports show low overpotentials; for example, approximately 89 mV at 10 mA cm^{-2} for HER in alkaline media. Thus, these composites will be able to compete with noble metal catalysts such as platinum. Similarly, OER performances have been enhanced. With such composites having low overpotentials, it is attributed to the optimized structure and electronic properties due to nitrogen doping. Active Sites - Embedding nitrogen functionalities into the carbon matrix enhances electron transfer kinetics, an essential feature for both the HER and OER processes. The presence of nitrogen species improves the adsorption energies of reaction intermediates, allowing for faster reaction kinetics. DFT studies show that the electronic interactions at the interface between Ni_3N and N-doped carbon further optimize the charge transfer processes during electrocatalytic reactions, increasing catalytic efficiency even more.
in conclusion hydrothermal and solvothermal methods are thus considered efficient techniques for synthesizing nickel nitride within a nitrogen-doped carbon matrix for their porous structures, which enhance catalytic activity toward OER and HER. Further investigation in this area will be related to the optimization of synthesis techniques, which will further improve the performance of Ni_3N@N-C composites in renewable energy technologies [84,90,116,117].

2.5 Electrocatalytic Performance of Non-noble materials

2.5.1 Overpotential

Overpotential is herein defined as the additional voltage required by the theoretical value, which drives the electrochemical reaction at a certain rate. It is a crucial parameter in the efficiency assessment of electrocatalysts with respect to both OER and HER. Theoretically, the OER process has a minimum overpotential of about 0.3 to 0.4 V because of the way the oxygen-containing intermediates (*OH, *O, and *OOH) scale with each other [118].

Indeed, recent efforts have been made to utilize nickel-based electrocatalysts for water splitting reactions; the overpotential values are varying for OER and HER. For example, the Ni nanoparticles encapsulated by N-doped carbon (Ni@N-C) demonstrated low overpotentials of 117

mV for HER and 325 mV for OER [12]. The core-shell structures of Ni@Ni-NC displayed an OER overpotential of 371 mV, surpassing that of the commercial benchmark IrO_2 [119]. Nickel nitride (Ni_3N) on Ni foam has shown excellent HER activity in alkaline solution, with an overpotential of ~50 mV[100]. This was explained because the "in situ" formation of a $Ni(OH)_2$ layer on the nitride surface occurred. The nitrogen-doped carbon encapsulation around γ-MoC/Ni heterostructures resulted in γ-MoC/Ni@NC, exhibiting an OER onset overpotential of 240 mV and an overpotential of 310 mV at 10 mA cm^{-2} [120]These studies highlight that these nickel-based materials can serve as active electrocatalysts for water-splitting reactions\

Table 2. 5 Summar for overpotential of nickel-based materials as efficient electrocatalysts for water splitting,

Electrocatalyst	**Reaction**	**Overpotential (mV)**	**Current Density (mA cm^{-2})**	**Ref.**
Ni@N-C	HER	117	10	[12].
Ni_3N on Ni Foam	HER	~50	-	[100].
Ni@N-C	OER	325	10	[12]
Ni@Ni-NC	OER	371	10	[119]
γ-MoC/Ni@NC	OER	310	10	[120]

These findings underscore the potential of nickel-based materials as efficient electrocatalysts for water splitting, showcasing their effectiveness in both HER and OER applications.

2.5.2 Over potential and Tafel slope

Recent studies have stated the activity of a number of electrocatalysts in view of their overpotential and Tafel slope values concerning water splitting reactions. In the oxygen evolution reaction, the typical overpotential was reported for nickel nanoparticles encapsulated in nitrogen-doped carbon at a Tafel slope of 123 mV/dec [121]. In sharp comparison, much lower Tafel slopes are shown by

[110]NiCo alloy catalysts at 50.1 mV/dec, though overpotential data reported for the said catalyst has not been indicated.

In the case of HER, the overpotential of Ni-NC was 263 mV with a Tafel slope of 145 mV/dec. For the NiCo alloy, exhibited a Tafel slope of 83.9 mV/dec, but again, the value of overpotential was not provided. In addition, γ-MoC/Ni@NC composite showed a promising OER performance with overpotential as low as 240 mV, though its Tafel slope was not mentioned (Zhang et al., 2017)

The most recent research has focused on the development of active, noble metal-free electrocatalysts for both OER Several types of materials have shown promising performance, including FeCoNi alloy with overpotential of 400 mV for OER and with Tafel slope of 72 mV/dec as investigated by [122] and Ni-Co oxides displaying the dual Tafel slope behavior in [123]. Among them, heterostructured γ-MoC/Ni encapsulated in N-doped carbon showed an excellent performance toward OER with an onset overpotential of 240 mV.

Very recently, a catalyst with bimetal Mo-Ni/NC displayed excellent activity toward OER. For the OER, an overpotential of 270 mV was achieved with a current density of 10 mA/cm2 and a Tafel slope of 64.3 mV/Dec [124]. These studies reveal the potentiality of non-precious metal catalysts toward improvement in water electrolysis and related energy conversion technologies by offering alternatives to the costly noble metal-based catalysts. On one hand, such findings could indicate the potential of nickel-based electrocatalysts for improving the efficiency of the water splitting process.

Table 2. 6 Summary for Tafe slope as potential of nickel-based electrocatalysts for improving the efficiency of the water splitting process.

Reaction	**Electrocatalyst**	**Over Potential (mV)**	**Tafel Slope (mV/dec)**	**Reference**
OER	Ni@N-C (Nickel Nano par ticles in N-Doped Carbon)	325	123	[121].
OER	NiCo Alloy	-	50.1	[121].

HER	Ni-NC (Nickel Nano part - icles in N-Doped Carbon)	263	145	[121].
HER	NiCo Alloy	-	83.9	[121].
OER	γ-MoC/Ni@NC	240	-	-
HER	Fe-Doped Ni_3C in N-Doped Carbon	~50	-	[110]
OER	Ni/Fe_3O_4 Heterostructures	296	61	[125]
OER	$NiCo_2O_4$/NiO Hollow Microrods	-	-	[126]
OER	FeCoNi Alloy	400	72	[122]
OER	Ni-Co Oxides	-	Dual Tafel slope	[123]
OER	γ-MoC/Ni@NC	240	-	[120]
OER	Mo-Ni/NC Bimetal	270	64.3	[124]

2.5.3 Electrochemical Impedance Spectroscopy (EIS)

While nickel-based nanoparticles act as bifunctional electrocatalysts toward OER, catalysts of this type in general exhibit very high activities, stabilities, and durability compared to noble metal catalysts in alkaline mediums[127–129].The doping of nitrogen into the carbon matrix, confirmed by different spectroscopic techniques, has improved the catalytic performances due to the modification of electronic properties of the material. Their excellent performance might be attributed to the unique three-dimensional hierarchical structure, including uniformly distributed metal nanoparticles encapsulated by a partially graphitized N-doped carbon shell. Several important parameters explaining the improved catalytic activity of these nitrogen-doped carbon materials, such as density of states, carrier concentration, and flat band potential, have been derived

using electrochemical impedance spectroscopy. The following table summarizes the electrochemical impedance spectroscopy (EIS) data for various non-noble electrocatalysts, focusing on the resistance and capacitance parameters: R1/RS, C2/CPEdl, R2/Rct, R3/Rf, and C2/CPEf.

Table 2. 7 Provide insights into the EIS electrochemical performance and characteristics of some selected materials.

Electrocatalyst	**R1/RS (Ω)**	**C2/CPEdl (μF/cm²)**	**R2/Rct (Ω)**		**R3/Rf (Ω)**	**C2/CPEf (μF/cm²)**	**Ref**
Ni@N-C	10	1.5	25		15	0.8	[130]
NiCo Alloy	5	2.0	30		10	1.0	[130]
Ni-NC	12	1.8	20		12	0.9	[130]
Fe-Doped Ni_3C in N-Doped Carbon	8	2.5	18		14	1.2	[130]
γ-MoC/Ni@NC	6	1.0	22		11	1.5	[130]
Ni/Fe_3O_4 Heterostructures	9	1.7	24		13	1.3	[130]
FeCoNi Alloy	15	2.3	35		16	0.7	[131]
Mo-Ni/NC Bimetal	11	1.9	26		12	1.1	[132]

2.5.4 Stability of Electrocatalyst

Using potentiodynamic or Chronoamperometry techniques for measuring the change in voltage with time, or chronopotentiometry to detect the change in current over time, stability may typically be determined in several hours of measurement. The activity curve is then used to determine the level of stability. To improve stability even further, it's vital to first comprehend the chemical and physical activities that take place on the catalyst surface during reactions [28,29].

The table below summarizes the stability and performance metrics of non-noble Ni_3N composite electrocatalysts

Table 2. 8 Data on Non-Noble Ni_3N Composite Electrocatalysts and Their Stability

Electrocatalyst	Current Density (mA/cm^2)	Over potential (η) (mV)	Stability Duration	Comments/ Performance Highlights	Ref.
Ni_3N-CeO_2/NF	50	350	40 h	Maintained performance with low overpotential for OER	[98]
Ni_3N/NF	20	Not specified	24 h	Potential drop of ~95 mV over 24 h; stable activity post-test	[133]
Ni_3N-2CeO_2/NF	10	42	Not specified	Optimal performance for HER with significant stability	[98]
Ni_3N/$Ni(OH)_2$-NiOOH	50	7.6	50 CV cycles	Improved HER performance after CV cycling; stable activity	[133]
NiFeN@NiMoN Core-Shell	500	369	Not specified	Excellent durability for seawater electrolysis; high current density achieved	[134]

2.6 Summary on Challenges and Limitations of Nickel Nitride Based Electrocata list for OER and HER

The nitrogen-doped carbon-supported nickel nitride-encased Ni_3N has a lot of potential to be a very useful electrocatalyst for both OER and HER reactions. However, there are many challenges and limitations toward effectiveness and utilization.

2.6.1 Stability Problems

The structural deterioration in Ni_3N after a very long period of electrochemical cycling can occur and thus seriously weaken the catalytic activity. More precisely, this is realized under harsh conditions typical of the OERs, whereby the formation of surface oxides can change the active site and decrease the overall efficiency [133]. The nitrogen-doped carbon support itself may degrade overtime, especially at high temperatures or in aggressive electrolytes. This leads to a loss of structural integrity as well as catalytic performance [100].

2.6.2 Kinetic Limitations

Although Ni_3N exhibits lower overpotentials compared with some of the traditional catalysts, it needs a high input of energy to realize high current densities. For instance, its overpotential in HER may go as high as 171.9 mV at a certain current density, which is higher than in noble metal catalysts like platinum[90]. The kinetics of both OER and HER may be significantly controlled by sluggish electron transfer processes across the interface between Ni_3N and the electrolyte. This can impede the overall efficiency of these reactions, especially under different pH conditions[100].

2.6.3 Variability in Electrocatalytic Activity

The performance of Ni_3N is sensitive to the degree of nitrogen doping in the carbon matrix. It requires an optimum for the enhancement of electronic properties, while the structural stability has to be sacrificed. Either too little or too much nitrogen might provide suboptimal catalytic behavior. Surface oxidation may form either $Ni(OH)_2$ or NiOOH layers; such a process could block the active sites or even change the reaction pathways during operation, thus leading to gradual loss of activities[90].

2.6.4 Environmental Sensitivity

The performance of Ni_3N encapsulated in nitrogen-doped carbon has much dependence on the use of different electrolytes, such as alkaline or acidic. Limitations of this system can be less versatile and may require careful selection in applications based on needs [90]. Impurities of iron ions can be present in alkaline solutions, which affect catalytic activity. Such impurities may further complicate optimization by either increasing performance or acting as inhibitors [133]. Although nitrogen-doped carbon encapsulating nickel nitride is suitable for both OER and HER, there are still challenges yet to be overcome because of the stability of operational conditions, kinetic limitations, variations in electrocatalytic activity, and environmental sensitivities. Further research has to be carried out to improve the structural integrity of NQN@NCFP by controlling the optimal doping level, so finding the reaction mechanisms becomes a key factor in improving its electrocatalytic performance.

3. MATERIALS AND METHODS

3.1 Materials

The metallic-Ni powder particles, NH_3 and N_2 gases, 3.5 mg mL^{-1} of dopamine hydrochloride, 10 × 10^{-3} M tris buffer (tris (hydroxyl methyl) amino methane)), deionized (DI) water, ethanol, 2.263 mmol thiourea and 60 mL Teflon-lined stainless-steel were used. This is a mixture of metallic nickel powder, ammonia, nitrogen gas atmospheres, dopamine hydrochloride, tris buffer, deionized water, ethanol, thiourea, and an appropriate reactor lined with Teflon along its inner walls made from stainless steel. Such a well-formulated combination is aimed at nanoparticles or catalysts for the synthesis of nickel nitride core and nitrogen doped carbon shell. Each component has been chosen because of the role it can play, given that it facilitates chemical reactions while ensuring the stability and properties of the desired material. NH_3 acts as a precursor, providing nitrogen to the nickel nitride formed in the synthesis reaction. N_2 provides an inert atmosphere, ensuring that no oxidation takes place and the synthesis is stable. Significance: In fact, the mixture of these two gases is crucial to developing the reducing atmosphere needed for the formation of Ni_3N.

3.2 Methods

3.2.1. Preparation of PDA Coated Nickel

Polydopamine was first coated on metallic Ni powder to form a uniform layer so as to enhance the nitridation as shown in figure 3.1. The oxidative polymerization of the dopamine hydrochloride was then stimulated by pH in an alkaline solution at pH 8.5, coating the nickel powder with a shell of PDA. Aqueous solutions of dopamine hydrochloride were prepared at various mass ratios relative to metallic Ni powder, namely, 1:1, 1:1.41, and 1:2.0. The concentration of DA hydrochloride was kept at 3.51 mg/mL in the solution of 10 mM Tris buffer. To this regard, the metallic Ni powder was dispersed into the DA solution prepared for a while to distribute uniformly in the solution. The resulting mixture was then stirred at room temperature for 24 h. With such a long stirring time, a thin, uniform layer of PDA can be obtained on the surface of the Ni particles. The ideal coating was produced when the mass ratio of the dopamine hydrochloride to the nickel

was 1:2, while any other combination resulted in severe PDA aggregation. The coating acted like a precursor to further chemical modifications with the aim of enhancing stability and reactivity for the nickel particle. This will further prepare the metallic Ni for successive process steps of annealing and nitridation, hence yielding the desired nitrogen-doped nickel nitride structure [135–137].

3.2.2. Synthesis of core-shell PDA-Nickel Structure

4 M HCl solution was used for etching PDA coated nickel, as this concentration will sufficiently serve in the partial removal of nickel to get core shell PDA-nickel structure. The etching was done for varying time intervals: 30, 45, and 60 minutes. Each time period allowed for a detailed study of how the etching time affects the structural and electrochemical properties of the Ni-PDA particles. 45 minutes was obtained to be the optimum etching time. By introducing void space between the nickel core and the cloth portion of the PDA shell, the Ni-PDA inner sheath's reduction during etching was achieved. Finally, after 45 minutes of etching, the Ni-PDA particles are washed with DI water and ethanol to remove residual acid and byproducts of the reaction.

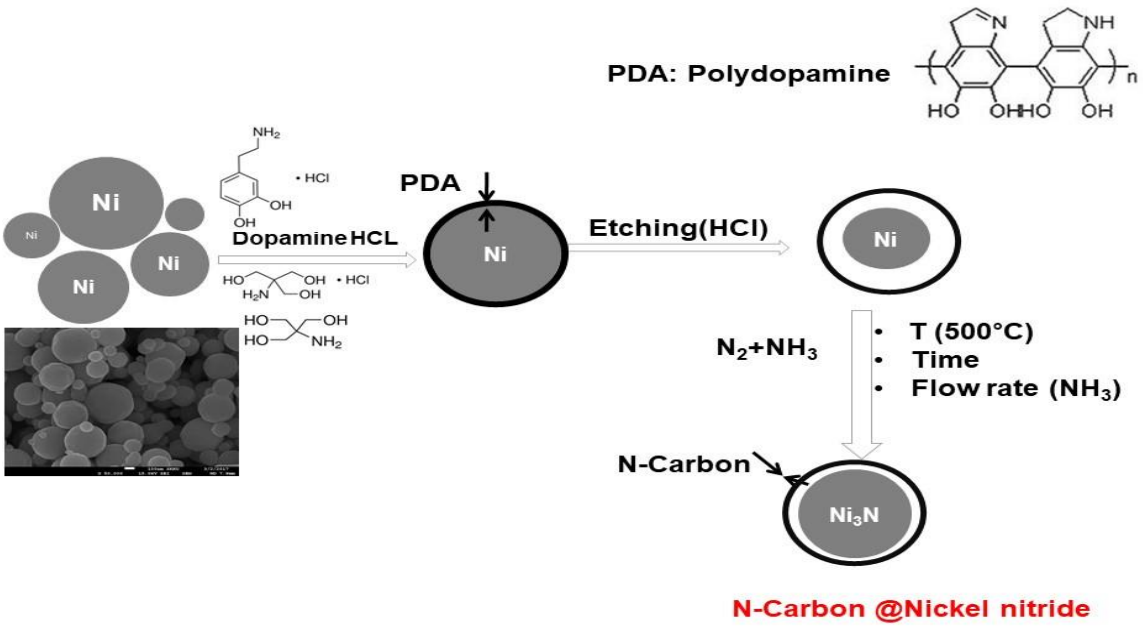

Figure 3. 1 Schematic representation for the synthesis of (Ni_3N@NC

3.2.3 Synthesis of Nickel Nitride-Nitrogen Doped Carbon Core-Shell Structure

The annealing process is thereafter performed to convert Ni-PDA into nitrogen-doped carbon-coated metallic nickel particles (Ni-NC). Particles of Ni-PDA are taken in a high-temperature furnace capable of maintaining controlled atmospheres. Here, an inert atmosphere was created with a mixture of gases, including ammonia (NH_3) and nitrogen (N_2). Therefore, the primary role of this mixture was to provide the proper atmosphere for the desired annealing chemical transformations, nickel to nickel nitride and carbon to nitrogen doped carbon. Annealing is done at 500 °C for 3, 6, 12, and 24-hours. This temperature is selected to provide conditions for the thermal decomposition of PDA into nitrogen-doped carbon. Annealing for different periods allows the time effects on the properties of resulting Ni-NC particles to be systematically investigated. Upon attainment of 500 °C, the PDA coating starts its thermal decomposition that, in turn produces a layer of nitrogen-doped carbon around the metallic Ni particles. The NH_3 atmosphere acts as an agent that helps introduce the nitrogen into the nitrogen doped carbon matrix that improves the properties of carbon and increases stability. At less period of nitridation and low flow rate of NH_3 and N_2 there is no more formation of Ni_3N started to appear. Nevertheless, a long nitridation and high flow rate promote the formation of more Ni_3N. With increasing duration of nitridation, N_2 and (NH_3) gases were gradually released, it then reacted with the metallic Ni core in the Ni–NC Core Shell to form Ni_3N@NC Core Shell and NH_3.

The cooling of the furnace is carried out to room temperature under an inert atmosphere after the scheduled time for annealing, in order to avoid the oxidation of newly formed Ni-NC particles. The product from this step includes nitrogen-doped carbon-coated metallic nickel particles, Ni-NC, displaying excellent electrochemical properties owing to their unique structure and composition.

3.3 Material Characterization

Raman spectroscopy was used to identify the different phases of carbon in the N-doped carbon shell. The alpha300 M+ system was used to excite the sample with a laser; the photons scattered inelastically to result in a spectrum representative of the molecular vibrations in the sample.

A 532 nm laser was found to work quite well for many organic compounds or material because it seemed to yield a good Raman signal. XRD was used to confirm the presence of characteristic peaks associated with the Ni_3N phase. The 7500F FE-SEM (FE-SEM; JEOL, Japan) was used to assess the surface morphology. TEM and HR-TEM (200 kV) were used to analyze the microstructures of the hybrid structure. EDS elemental mapping under the scanning TEM (STEM) and XPS were employed to study the NiS– NC HS composition.

The linear-sweep voltammetry with a scan rate of 1 $mV \cdot s^{-1}$ and cyclic voltammetry in 1 M KOH were conducted on a CHI 660D (CH Instruments, Inc., Austin, TX) electrochemistry work station using a three-electrode cell. Hg/HgO (1 M NaOH) and Pt wire electrodes were used as reference and counter electrodes, respectively. The working electrodes were prepared by mixing the as-prepared active materials (Ni_3N@NC), Ketchen black, and poly vinylidene difluoride with a mass ratio of 7:2:1 in N-methyl-2-pyrrolidone. A piece of carbon paper was taken and cleaned from any contaminant. Carbon paper, 1cm x 1cm in dimensions was used to coat the Ni_3N@NC slurry. The slurry was coated uniformly on one side of the carbon paper using doctor blade. The coated carbon paper was placed in a vacuum oven at 90 °C and dried overnight, for about 12 hours. This is to ensure that adequate adhesion of materials was achieved and complete elimination of solvent. The catalyst loading for Ni_3N@NC was approximately 2.6 $mg \cdot cm^{-2}$. Electrochemical impedance spectroscopy (EIS) measurements was conducted using a three-electrode system with frequency range 100 kHz–0.1 Hz, and amplitude of applied voltage was 5 mV. The stability of mesoporous Ni_3N@NC was conducted in 1 M KOH by applying a static current density of 20 $mA \cdot cm^{-2}$.

4. RESULTS AND DISCUSSIONS

Raman spectroscopy was verified the nitrogen doping in carbon, reflecting both its graphitic and amorphous forms. XRD confirmed the efficient synthesis of the material with no loss of crystallinity and the phase purity of nickel nitride. TEM showed that catalysis has particles of uniform size. HRTEM confirmed the correct lattices of nickel nitride as being crystalline with negligible amorphization. In the end, it was revealed that the Ni-NC catalyst proves to be highly efficient in electrocatalysis under alkaline conditions and such that is characterized by fast charge transfer kinetics with negligible charge transfer resistance. Raman spectroscopy indicated nitrogen-doped carbon with the coexistence of graphitic and amorphous structures; from the intensity ratios, a high degree of nitrogen doping was estimated that would enhance the electronic properties of the catalyst. The XRD analysis indicated sharp peaks of nickel nitride phases without losing crystallinity or phase purity during the synthesis. TEM showed a homogeneous dispersion of the nickel nitride nanoparticles within the nitrogen-doped carbon matrix, which is of prime importance for catalytic behavior. Further detailed images of the crystalline lattice structures of nickel nitride with minimal amorphization upon encapsulation were further demonstrated by HRTEM. With performance evaluation, the catalyst Ni-NC had an overpotential of 292.28 mV under alkaline conditions at a current density of 10 $mA \cdot cm^2$ for hydrogen evolution; this confirms high electrocatalytic efficiency due to the low overpotential. The Tafel slope revealed rapid charge transfer kinetics, which indicates that the catalyst is efficient in promoting the electrochemical reaction.

Moreover, electrochemical impedance spectroscopy data confirmed low charge-transfer resistance, clearly allowing the conclusion to be drawn that this Ni-NC structure supports fast electron transport, responsible for the maintenance of a high catalytic performance over time.

4.1 Characterization of Ni_3N@NC

Nitrogen doping in carbon was verified by Raman spectroscopy, which showed peaks indicating graphitic and amorphous forms. High intensity ratios suggested a substantial nitrogen doping, which enhanced the catalyst's electrical properties even more. The effective production of the material was demonstrated by sharp peaks by X-ray diffraction (XRD) attributed to the crystalline phases of nickel nitrides. These peaks also indicated that encapsulation preserves the crystallinity

and phase purity of nickel nitride. A homogenous dispersion of Ni_3N nanoparticles in an N-doped carbon matrix was observed by Transmission Electron Microscopy (TEM), which also verified the consistent particle size for catalysis. While EDX demonstrated effective encapsulation by assessing elemental composition, STEM offered high-resolution images of the encased particles. The precise lattice structures of nickel nitride were ascertained by HRTEM, which also demonstrated that the material is crystalline with very little amorphization in encapsulation. It provided details on the surface chemical states of nitrogen and nickel and demonstrated that strong interactions between nitrogen-doped carbon and nickel nitride enhance catalytic activity because of different nitrogen functions.

4.1.1 X-Ray Diffraction Analysis for Phase identification and crystallinity

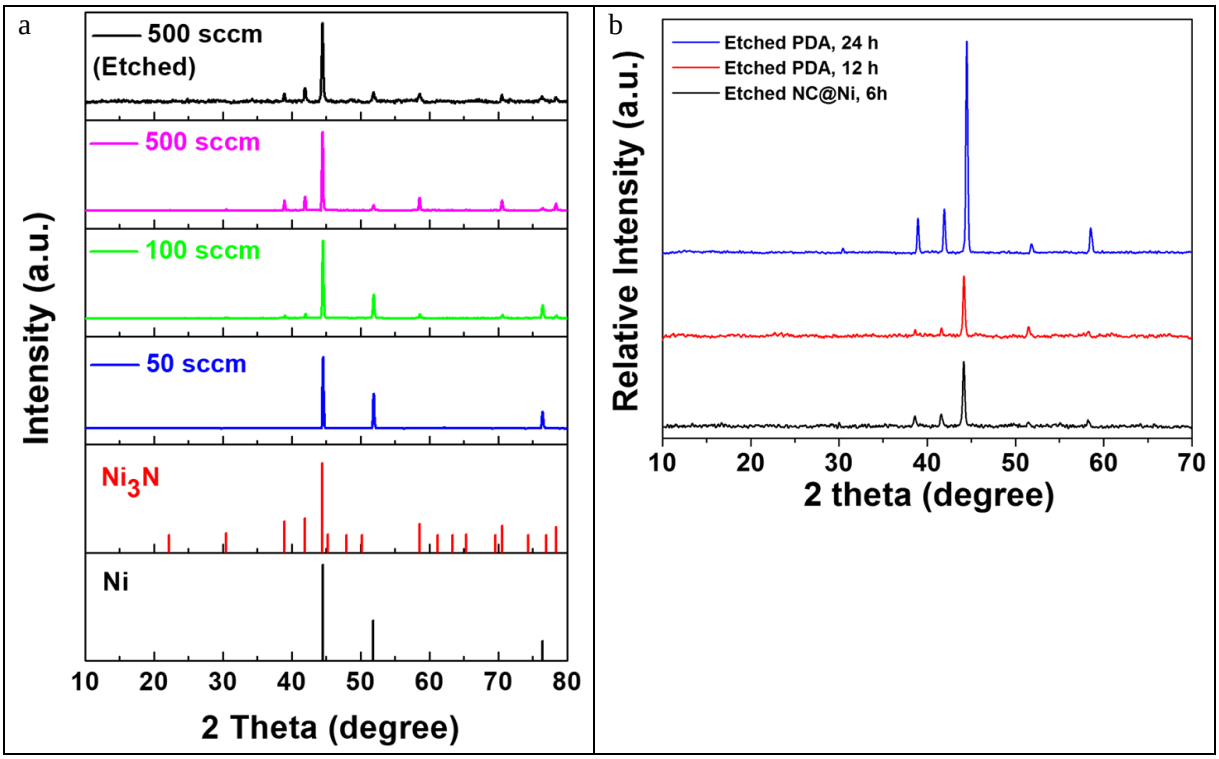

Figure 4. 1 (a) XRD patterns of Ni3N@NC prepared at different flow rates (b) relative intensities

The XRD patterns of the Ni_3N@NC structures synthesised at different ammonia flow rates are shown in Figure 4.1 (a). The recorded diffraction patterns indicate that the samples are not single-

phase. All experimental Ni_3N@NC samples successfully achieved highly crystalline nickel nitride (Ni_3N) phases[18]. The characteristic XRD peaks at $2\theta = 44.5^0$, indexed to the (111) plane, were observed in the standard data from JCPDS 04-004-2240[138]. At a lower ammonia flow rate of 50 sccm, the Ni phase exhibited diffraction peaks at $2\theta = 52^0$ and 76^0, corresponding to the (200) and (220) planes, respectively[139]. The presence of sharp peaks and the absence of Ni peaks—which would complicate the identification of pure nitride phases—demonstrate the enhanced crystallinity of Ni_3N in the Ni_3N@NC electrocatalyst. Figure 4.1 (b) shows the relative intensity of etched Ni_3N@NC samples at different durations: PDA-24 h, PDA-12 h, and NC-Ni-6 h. It is evident that Ni particles were removed during the etching process to facilitate the formation of the Ni_3N phase. While the Ni_3N core phase at $2\theta = 44.50$ is preserved, other phases may also emerge alongside observable phase changes due to etching. The varying etching outcomes highlight the importance of both the NC shell and void space in developing an effective core shell structure that prevents neighboring particles from aggregating across different phases [139]. The relative intensity of diffraction peaks for etched PDA after 24 hours compared to those formed after 12 hours indicates that higher crystalline phases of Ni_3N in the Ni_3N@NC composite result from a higher ammonia flow rate. This promotes the formation of a core within the NC shell that can withstand molecular nitrogen removal, although it may also reduce the thickness of the NC shell. However, etching in both PDA-Ni 6h and NC-Ni 6h samples resulted in a decrease in spectrum intensity that was even lower than that observed in their unetched counterparts [140].

4.1.2 Raman Spectroscopic analysis for Bonds on Ni-PDA and Ni-NC

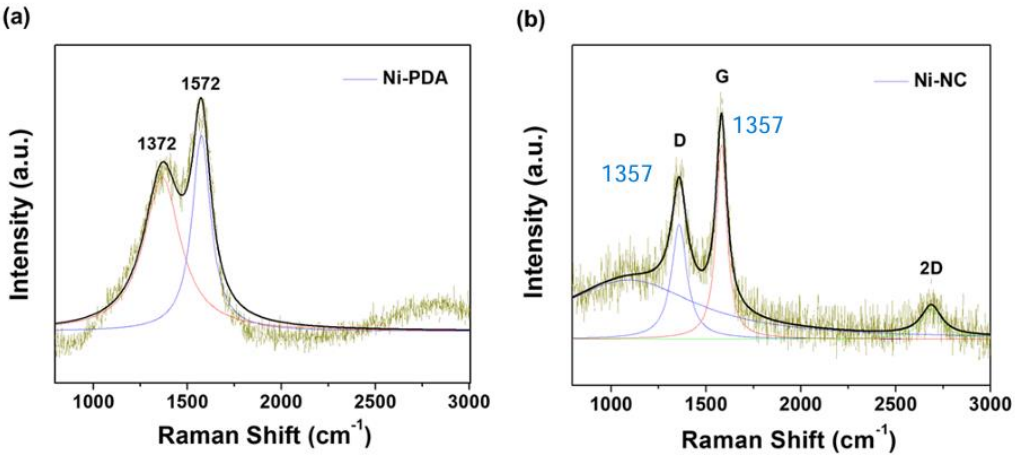

Figure 4. 2 Raman spectra of (a) Ni-PDA and (b) Ni-NC

The creation of the PDA and its conversion into the NC were verified using Raman spectroscopy. Figure 4.2 depicts the Raman spectra of N-PDA and N-NC. The N-PDA displays two peaks at 1572 and 1372 cm^{-1}, which are the result of the PDA stretching and deforming aromatic rings, respectively. Correspondingly, bands at 1357 and 1581 cm^{-1} presented in the Ni-NC bond are attributed to the D-band (sp^3-hybridised) and G-band (sp^2-hybridised), which are related to the vibrational bond of dangling of the C atoms in the edge-ending plane of the disarrayed graphite and the sp^2-hybridised C atoms in a 2D hexagonal lattice, respectively [141].

4.1.3 Transmission Electron Microscopies for composition and structural analysis

Strong proof that the anticipated core-shell structure was successfully constructed is provided by the TEM and scanning TEM (STEM) images in Figures 4.3 (a) and 6(c), which clearly distinguish the Ni_3N core from the NC shell. Individual nanoparticles were characterized using high-resolution transmission electron microscopy (HRTEM), which revealed that the lattice fringes are different from the nanosheet's, as shown in Figure 4.3 (b). The measured d-spacing of 0.2078 nm for the 111 planes of the hexagonal close-packed (hcp) structure is in good agreement with the anticipated values for Ni_3N, which correspond to the 111 facets seen at $2\theta = 44.50$ in the XRD spectrum. Furthermore, as can be observed in the STEM photos, figures S1 (a–f) show that the Ni_3N core is smoothly encased by the NC shell, indicating a robust contact between the core and shell.

Figure 4.3 (a, c)'s TEM and scanning TEM (STEM) pictures demonstrate the striking contrast between the Ni_3N core and the NC shell, providing additional evidence that the planned core-shell structure was successfully constructed. High-resolution Individual nanoparticles were characterized using TEM (HRTEM), and the lattice fringes differed from those of the nano sheet Figure 4.3 (b)). The (111) planes of hexagonal close packed (hcp) had a measured d-spacing of 0.2078 nm that was in good agreement with that measurement. Ni_3N which is consistent with (111) facets of Ni_3N corresponding to $2\theta = 44.5^0$ in X-RD data spectrum. Moreover, image S1 (a-f) for The Ni_3N core is smoothly bound by the NC shell, according to TEM (STEM), demonstrating a strong contact between the core and shell.

4.1.4 Energy Dispersive Spectroscopic analysis of elemental composition and distribution

Figures 4.3 (d) to 6(f) display the comparative distribution of the elements Ni, N, and C as determined by the EDS mapping results. These elements are evenly distributed throughout the Ni_3N@NC structure. The bright red areas on a black backdrop in Figure 4.3 (d) represent the elemental mapping of Ni in the core surrounded by the NC shell. The mapping of the nickel element in Figure 4.3 (e) reveals that the bright, light blue regions correspond to the same nitrogen distribution in the shell. One can observe that a black structural image of the core in Figure 4.3 (f), the elemental mapping for carbon, indicates that there is no carbon present. The bright green areas in the carbon elemental mapping correspond to the dark areas in the nickel elemental mapping.

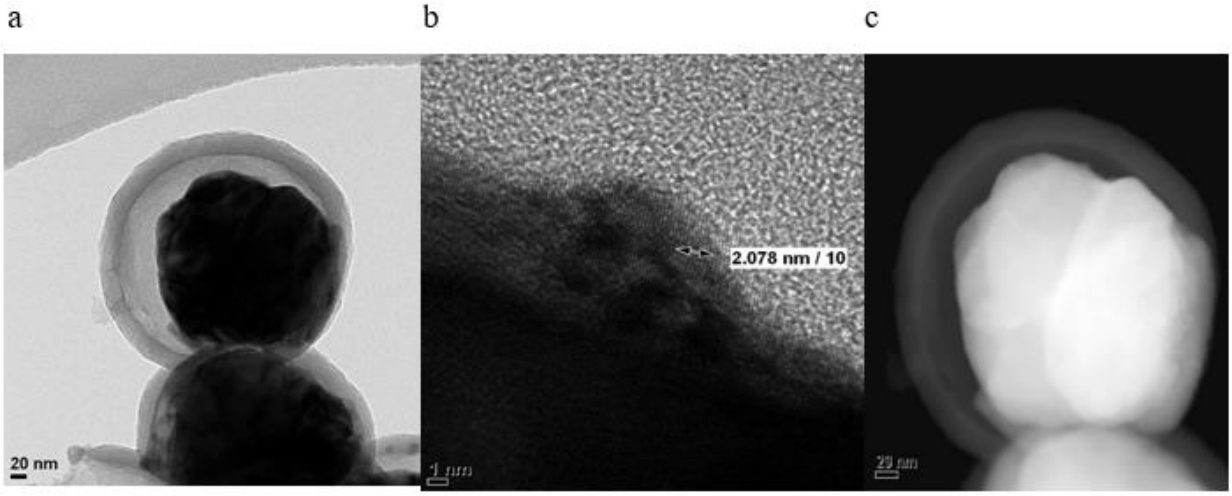

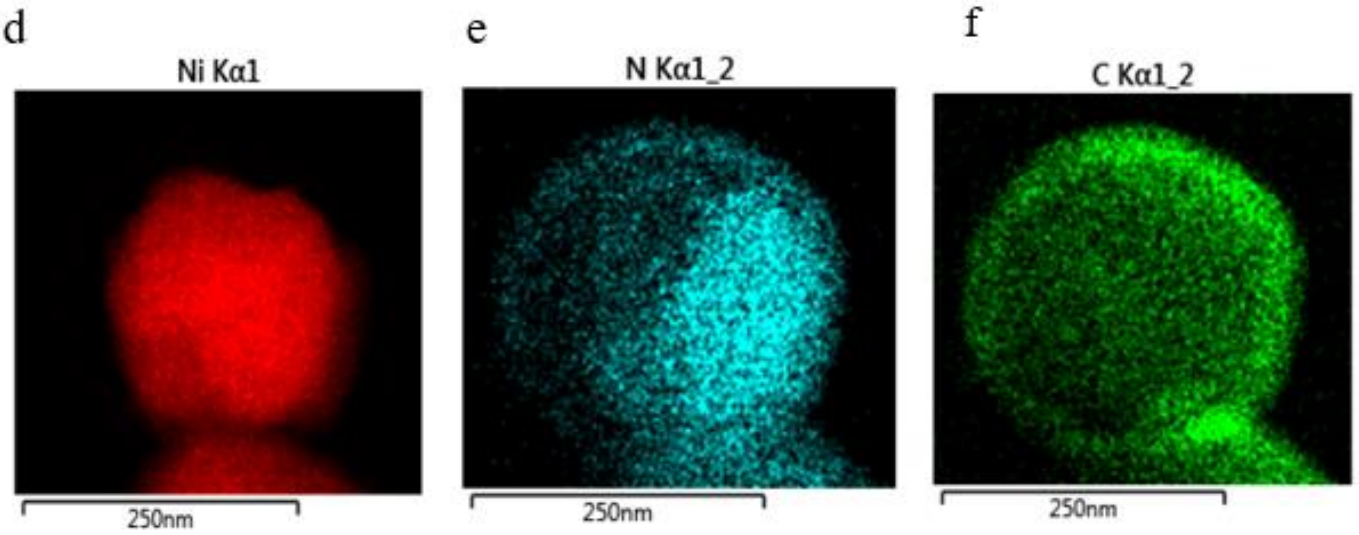

Figure 4. 3 (a) TEM, b) HR-TEM, c) STEM and (d-f) EDX elemental mapping of Ni_3N@NC-24h

4.1.5 X-Ray Photoelectron Spectroscopic analysis for elemental composition and chemical state

X-ray photoelectron spectroscopy (XPS) measurements were used to further investigate the chemical states and surface composition of the synthesised nitrogen-doped carbon shell surrounding a nickel nitride core structure, Ni_3N@NC. Figure 4.4 (a) XPS spectra of nickel nitride in the wide scan, showing the peaks for Ni, O, C, and N. Figure 4.4 (b) shows the metallic Ni particles in the low binding energy region at a range of 850-862 eV assigned to Ni 2p3/2 and four peaks in the high binding energy region at a range of 870-879 eV assigned to Ni 2p1/2. In the case of Ni_3N@NC-24, the presence of elemental Ni is verified by the two pronounced peaks at 852.6 and 870 eV. These correspond to XRD diffraction patterns, confirming that Ni exists in a monovalent oxidation state: Ni_3N; this is critical in catalyst formation. The peaks for Ni 2p3/2 at 854.5, 855.6, and 857 eV, along with corresponding peaks for Ni 2p1/2 at 872, 873, and 874 eV, suggest the presence of NiO, $Ni(OH)_2$, and NiOOH, respectively. These species likely arise from partial surface oxidation of the nitride that cannot be entirely avoided and are believed to be localised at the interface between the Ni_3N core and the NC film on the surface[142,143]. Furthermore, Figure 4.4 (c) presents the C 1s spectra, where SP^3 and SP^2-hybridized carbon correspond to three peaks at binding energies of 284.65 eV (C-C/C=C), 286.4 eV (aromatic C-N bonds), and C=O bonds [4,18].Figure 4.4 (d) displays the N1s XPS spectrum, revealing two distinct nitrogen species present in pure Ni_3N. The primary characteristic signal at 398.05 eV in the high-resolution N1s XPS spectra of Ni_3N@NC is assigned to nitrogen atoms coordinated to nickel atoms. Additionally, pyrrolic nitrogen is indicated by two peaks at 399 eV, suggesting the formation of an NC layer [144]. Figure 4.4 (d) shows the N 1s XPS spectrum, indicating that there are different nitrogen species in Ni_3N: a strong signal at 398.05 eV can be assigned to nitrogen atoms bound to nickel atoms. The contributions of pyrrolic-N are contained in two peaks at 399 eV, which also imply the growth of an NC layer. Further comparative tests under the same

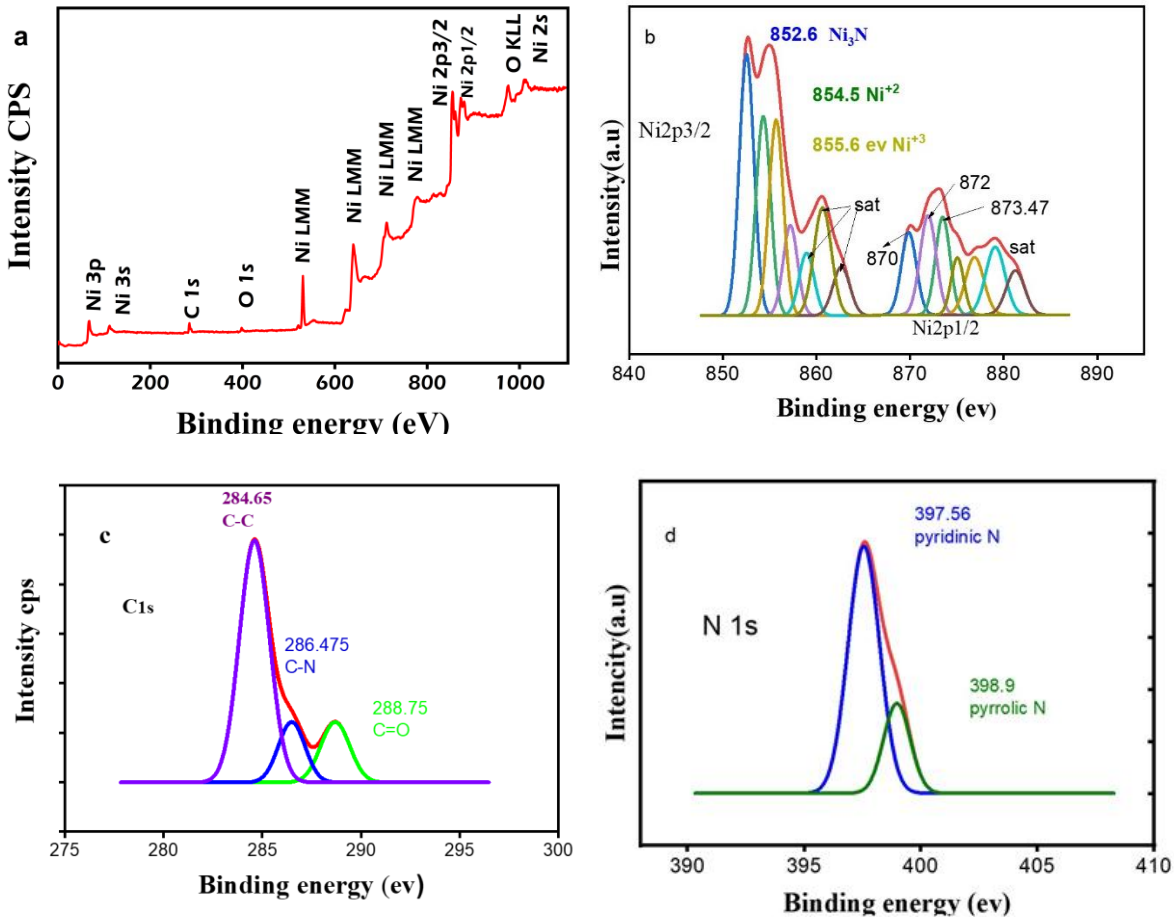

Figure 4. 4 XPS high-resolution spectra of Ni_3N@NC (a) wide spectra, (b) Ni_2p (c) C 1s, (d) N1s

conditions in carbon paper and IrO_2 underlined the performance of Ni_3N@NC during OER

4.2 Electrochemicalperformance measurements

It was also concluded that the nickel nitride-nitrogen-doped carbon complex showed better activity of water splitting with the hydrogen evolution rate improvement. Nitrogen-doped carbon-encapsulated nickel nitride had continuous activity for a very long period of time. Electron density was finely tuned, along with improved catalytic activity on account of the synergistic effect of the composite material. The overall electrocatalytic activity of the encapsulated materials had improved on account of improved current densities as well as electrocatalytic performance.

4.2.1 Overpotential

Figure 4.5 (a) shows the IR-corrected linear voltammetry (V) polarization curves, indicating that the electrodes realized by Ni_3N@NC present different current densities and reduced OER starting potentials with respect to the classic electrodes made of IrO_2 and carbon paper. The LSV curves suggest that Ni^{2+}/Ni^{3+} oxidation would occur at around 1.39 V vs. RHE, which is reversible according to the LSV of Ni_3N[17]. Compared to the Ni_3N@NC samples, Ni_3N@NC-24 showed the highest OER activity, with an onset potential of merely 1.522 V. At a current density of 10 $mA \cdot cm^{-2}$, it only needed an overpotential as low as 20 mV compared with IrO_2 (~292.8 mV), whereas samples that were tested at 3hr, 6hr, and 12hr required overpotentials as high as 365.6 mV, 365.4 mV, and 358.6 mV, respectively. These results suggest that the reduction of the thickness of the NC layer in Ni_3N@NC increases its activity as active sites become more accessible. The synergistic interaction in the coating of NC and Ni_3N drastically enhances the catalytic activity compared with pure Ni_3N [145]. A performance comparison of Ni_3N@NC-24h with IrO_2 underlined the critical role of encapsulation with NC in enhancing the OER activity of this composite material to become one of the most efficient electrocatalysts for water oxidation applications.

4.2.2 Tafel slope

Figure 4.5 (b) depicts the Tafel plots for all catalysts, which can provide broad insight on the reaction kinetics of Ni_3N@NC. To this end, the Tafel slopes for the electrodes Ni_3N@NC-24h, Ni_3N@NC-12h, Ni_3N@NC-6h, and Ni_3N@NC-3h were recorded at 110.68, 114, 153.5, and 183.56 mV dec^{-1}, respectively. These results indicate that the optimal OER kinetics were achieved at 24 hours for Ni_3N@NC-24h, as its Tafel slope is lower than those of single-phase Ni_3N (132 mV/dec) and Ni_3N/NC (125 mV/dec) reported by [57,146]. This significant difference in Tafel slope at lower potentials can be attributed to the unique core structure that enhances the specific surface area, facilitates interparticle porosity, and promotes the formation of NiOOH on the catalyst surface—an electrically active species [57,147]. This suggests that encapsulating an NC shell around a Ni_3N core can lead to improved OER rates. Conversely, as depicted in Figures 4.5 (d) and (f), the Ni_3N@NC-24h, 12h, and 6h samples exhibited excellent HER performance with an overpotential of approximately 143 mV, which is only 15 mV higher than the commercial Pt/C

catalyst's overpotential of 128.4 mV at a current density of 10 mA cm^{-2}. The Tafel plots associated with these polarization curves are shown in Figure 4.5 (b) and detail comprehensively the reaction path for HER on the electrocatalysts. The Tafel slope obtained for Ni_3N@NC-24h was given at a very low value of 65.26 mV dec^{-1}, which is 17.2 mV dec^{-1} higher than that of Pt/C (48.2 mV dec^{-1}) but quite higher than that of Ni foam of 190 mV dec^{-1} [148].

4.3.3 Charge transfer rate evaluation

The influence of the material's inherent features, such as charge transport and conductivity, on OER catalytic activity was further explored using electrochemical impedance spectroscopy (EIS) for Ni_3N@NC-24h. The EIS findings reveal that two key parameters affect the kinetic performance of an OER electrocatalyst: the charge-transfer resistance at the electrode-electrolyte interface and the internal resistance of the thin films. Consequently, Figure 4.5 (g) displays the Nyquist curve for Ni_3N@NC-24h fitted to an equivalent circuit model. The shortest semicircle in the Nyquist figure corresponds to the lowest contact and transfer impedance, which aligns with its greater OER activity. Table 5 displays the resistance values derived from the Nyquist plot, including the electrolyte resistance (Rs), charge transfer resistance at the electrode-electrolyte interface (RCT), and film resistance (Rf). The equivalent circuit fitting revealed that Ni_3N@NC-24h displayed the lowest charge transfer resistance (Rct) compared to Co0.21Ni0.25Cu0.54)3Se2, Cu3Se2, CoSe, and NiSe, indicating a quicker kinetic charge transfer rate at its thin film-electrolyte interface than that of binary selenides. This improved interfacial charge transfer can allow the quick synthesis of intermediates at the electrocatalyst surface, thereby decreasing the OER onset potential and resulting in high catalytic efficiency for Ni_3N@NC-24H.Similarly, charge transport inside the catalytic film is regulated by film resistance (Rf), which influences the overpotential at 10 mA cm2 and therefore impacts catalytic activity. A lower Rf value in Table 5 for the Ni_3N@NC-24h compared to the four binary compounds points to better conductivity within the thin layer. Insertion of Ni atoms into the lattice enhances intrinsic conductivity and is in excellent agreement with reduced film resistance. The higher charge transfer resistance across the electrode-electrolyte interface and the thin-film resistance, both enhanced by transition metal doping inside the catalyst, contribute to improved OER activity found for Ni_3N@NC-24h [3].

4.2.4 Stability Test Using chronopotentiometry.

The stability of Ni_3N@NC-24h was further determined during water oxidation using chrono potentiometry. From Figure 4.5 (h), the chrono potentiometric curve illustrates that the time-dependent overpotential on mesoporous Ni_3N@NC-24 at a constant current density of 10 mA/cm2 maintains stability for over 14 hours. Hence, it was clearly revealed that the mesoporous structure and unique structural features of Ni_3N@NC-24h enable long durability and provide a large number of catalytic sites with high stability in the course of the OER reaction. It was, however, found that the overpotential required for the Ni_3N@NC-24h to achieve a current density of 10 mA/cm2 was 370 mV, well below the 400 mV that has been reported in the case of Ni_3N/NC [18].

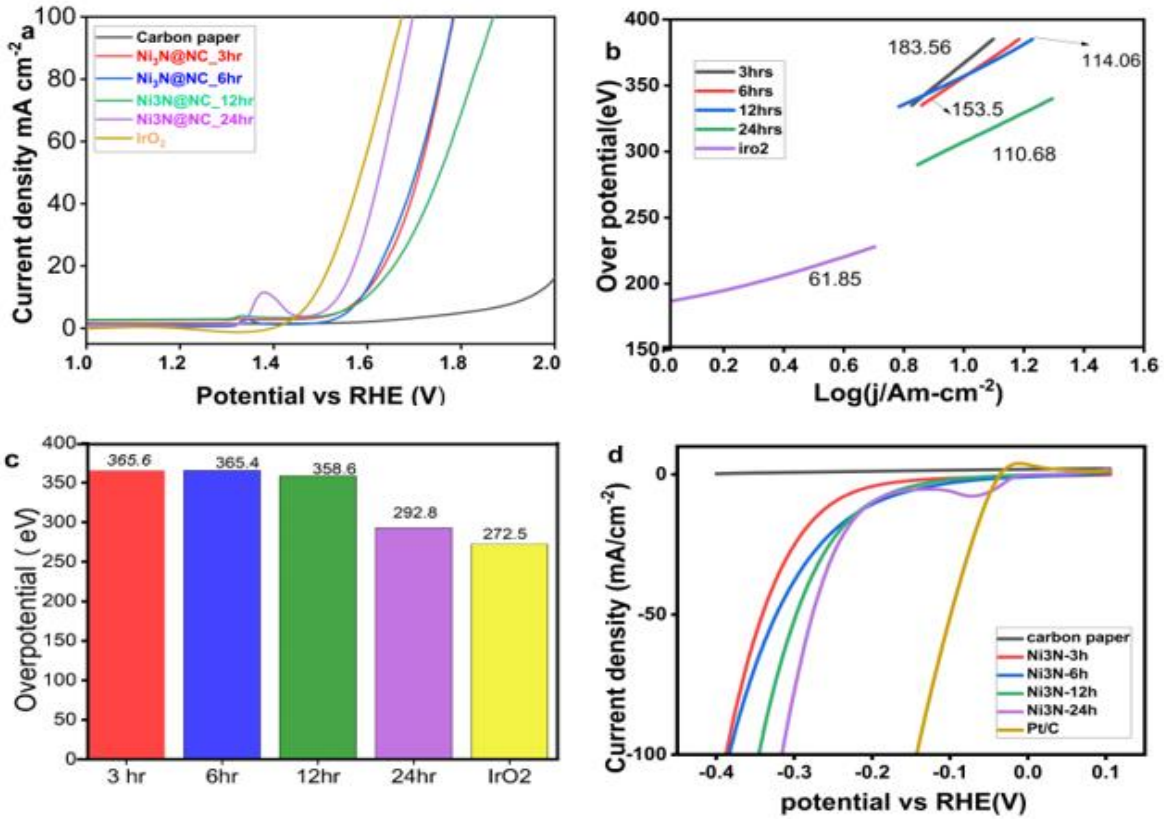

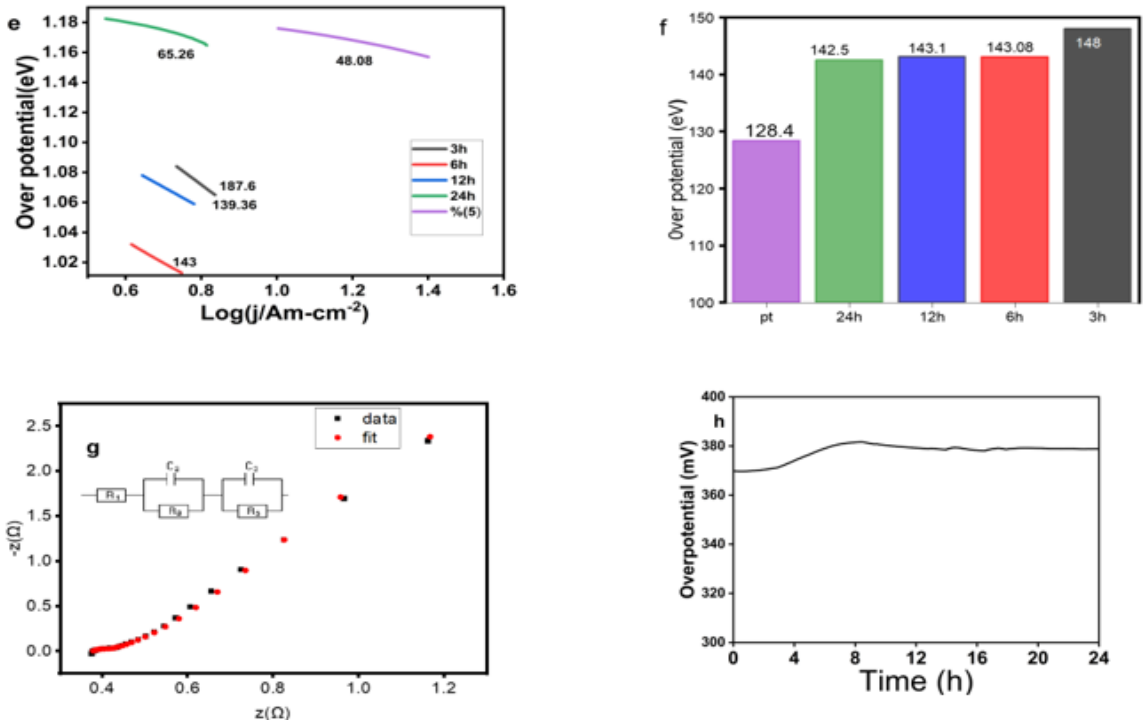

Figure 4. 5 Electrochemical measured properties in three-electrode configuration OER polarization curves in 1 M KOH at a scan rate of 5 mV s-1, the accompanying Tafel plots for all electrodes obtained as-is, a comparison of the over potentials needed to reach j=10 mA cm-2, HER polarization curves, and the associated Tafel plots of Ni_3N@NC are shown in (a), (b), and (c), respectively. (f) HER overpotential comparison (g) Nyquist plots for the OER performed at 2.5 V (versus. RHE); (h) Chronoamperometric responses at a constant 1.522 V (vs. RHE, Ej=10 of Ni_3N@NC-24 for 24 h in 1 M KOH and scale bar is 200 nm).

Table 4. 1 Equivalent circuit parameter obtained from fitting of EIS experimental data

catalyst	**R1/R_S**	**C_2/ CPEdl**	**R_2/Rct**	**R_3/Rf**	**C_2/ CPEf**
Ni_3N@NC -24hr	0.377 8 Ohm	3.744e-3 F	0.024 28 Ohm	16.09 Ohm	0.126 5 F
$(Co_{0.21}Ni_{0.25}Cu_{0.54})_3Se_2$	4.9	11.2	0.26	147.3	0.81
CoSe	5	14.2	.0.35	312.6	.83
Cu_3Se_2	5	18.4	0.48	1021.8	0.87
NiSe	5	279.1	0.66	1297.0	0.91

Rs represents electrolyte resistance; Rct represents electron transfer resistance; C1/CPEdl represents the constant phase element of double-layer non-ideal capacitance; Rf represents catalyst layer resistance; and CPEf represents capacitance. Rs represents electrolyte resistance; Rct represents electron transfer resistance; C1/CPEdl represents the constant phase element of double-layer non-ideal capacitance; Rf represents catalyst layer resistance; and CPEf represents capacitance.

5 CONCLUSIONS AND RECOMMENDATIONS

5.1 Conclusion

In conclusion, the oxygen evolution process in basic solution under mild conditions is being constructed and examined using the core shell structured Ni_3N-nanoparticles-encapsulated by nitrogen doped carbon nano surface sheath catalyst. Intriguingly, the core shell structure nitrogen doped Ni_3N@NC-24h catalyst shown enhanced activity and significantly better stability at 370 mV and over potential at 292.8 mV compared to the over potential of Ni_3N/NC at 400 mV and 310 mV, respectively. This catalyst produced a current density of 10 mA cm^{-2}. With a Tafel slope of 110.68 m V/dec, bringing about a noticeable difference in comparison to nickel foam Ni_3N. It was discovered that the NC shells and the purposefully left-over void space between the core and shell contribute significantly to the enhancement of the electrochemical performances by supplying a conductive channel that accommodates the Ni_3N particles and prevents their agglomeration. The good activity that has been seen may be attributed to the material's core shell structure, which increases the reaction surface area for electrocatalytic activity. The high stability was ascribed to Ni_3N's strong resistance to oxidation, which was demonstrated by XPS characterizations of aged catalyst and showed only very little surface oxide development.

5.2 Recommendation

Depending on the findings of this research the following recommendations are drawn as the following

Optimize the synthesis conditions to boost structural strength in Ni_3N, with an increased tolerance for the circumstances normal for OER. Alternative carbon supports or protective coatings should be explored, which ensure resistance against degradation at high temperatures and harsh electrolytes in order to sustain catalytic effectiveness over time.

Modify the structure or composition of Ni_3N by alloying or doping it in such a way that it decreases overpotential needs for both OER and HER. Elaborate on techniques of promoting quicker electron transport between Ni_3N and the electrolyte, such as surface modification or nanostructured materials for enhanced active surface area.

An appropriate nitrogen doping into the carbon matrix that is able to balance electrical benefits with structural stability for maximum catalytic efficiency will be sought. Emphasis must be given on investigations around the production of surface oxides such as $Ni(OH)_2$ or NiOOH and their influence on the active sites to result in novel techniques of sustaining catalytic activity.

Detailed investigations on the influences of various electrolytes on Ni_3N performance will be undertaken in view of optimum working conditions for every particular application. Development of ways for reducing impurities or contaminants, such as iron ions found in alkaline solutions inhibiting catalytic effectiveness.

The latter should provide explanations for design options aiming at enhanced electrocatalytic performance in reaction processes of OER and HER on Ni_3N. The procedures for stability and durability testing need to be systematically applied with a variety of operational conditions and assure that these findings are appropriate for applications.

REFERENCES

[1] Qu H Y, He X, Wang Y and Hou S 2021 Electrocatalysis for the oxygen evolution reaction in acidic media: Progress and challenges *Appl. Sci.* **11**

[2] Peng J, Dong W, Wang Z, Meng Y, Liu W, Song P and Liu Z 2020 Recent advances in 2D transition metal compounds for electrocatalytic full water splitting in neutral media *Mater. Today Adv.* **8** 100081

[3] Cao X, Johnson E and Nath M 2019 Identifying high-e ffi ciency oxygen evolution electrocatalysts from Co – Ni – Cu based selenides through combinatorial electrodeposition † 9877–89

[4] Kumar M, Jeong D I and Yoon D H 2020 Recent advances in 2D transition metal compounds for electrocatalytic full water splitting in neutral media *Electrochim. Acta* **333** 135545

[5] Gao M, Chen L, Zhang Z, Sun X and Zhang S 2018 Interface engineering of the Ni(OH)2-Ni3N nanoarray heterostructure for the alkaline hydrogen evolution reaction *J. Mater. Chem. A* **6** 833–6

[6] Jones B R 2024 e Role of Electrolysis in Green Hydrogen Production What Makes Electrolysis Essential for Green Hydrogen ? 1–5

[7] Song J, Wei C, Huang Z F, Liu C, Zeng L, Wang X and Xu Z J 2020 A review on fundamentals for designing oxygen evolution electrocatalysts *Chem. Soc. Rev.* **49** 2196–214

[8] Lyu F, Wang Q, Choi S M and Yin Y 2019 Noble-Metal-Free Electrocatalysts for Oxygen Evolution *Small* **15** 1–17

[9] Li C and Baek J B 2020 Recent Advances in Noble Metal (Pt, Ru, and Ir)-Based Electrocatalysts for Efficient Hydrogen Evolution Reaction *ACS Omega* **5** 31–40

[10] Xu H, Shang H, Wang C and Du Y 2020 Surface and interface engineering of noble-metal-free electrocatalysts for efficient overall water splitting *Coord. Chem. Rev.* **418** 213374

[11] Danilovic N, Subbaraman R, Chang K C, Chang S H, Kang Y, Snyder J, Paulikas A P, Strmcnik D, Kim Y T, Myers D, Stamenkovic V R and Markovic N M 2014 Using surface segregation to design stable Ru-Ir oxides for the oxygen evolution reaction in acidic environments *Angew. Chemie - Int. Ed.* **53** 14016–21

[12] Sun L, Zhuang G, Zeng S, Sha L, Zhan W, Sun L, Wang X and Han X 2021 Regulating the Electronic Structure and Active Sites in Ni Nanoparticles by Coating N-Doped C Layer and Porous Structure for an Efficient Overall Water Splitting *Inorg. Chem.* **60** 6764–71

[13] Xu Y, Tu W, Zhang B, Yin S, Huang Y, Kraft M and Xu R 2017 Nickel Nanoparticles Encapsulated in Few-Layer Nitrogen-Doped Graphene Derived from Metal–Organic Frameworks as Efficient Bifunctional Electrocatalysts for Overall Water Splitting *Adv. Mater.* **29** 1–8

[14] Ping X, Liu Y, Zheng L, Song Y, Guo L, Chen S and Wei Z 2024 Locking the lattice oxygen in RuO2 to stabilize highly active Ru sites in acidic water oxidation *Nat. Commun.* **15**

[15] Li G, Li S, Ge J, Liu C and Xing W 2017 Discontinuously covered IrO2-RuO2@Ru electrocatalysts for the oxygen evolution reaction: How high activity and long-term durability can be simultaneously realized in the synergistic and hybrid nano-structure *J. Mater. Chem. A* **5** 17221–9

[16] Zhao R, Li Q, Jiang X, Huang S, Fu G and Lee J M 2021 Interface engineering in transition metal-based heterostructures for oxygen electrocatalysis *Mater. Chem. Front.* **5** 1033–59

[17] Yuan Y, Zhou Y, Shen H, Rasaki S A, Wang J, Wang C, Wang J and Yang M 2018 Holey Sheets of Interconnected Carbon-Coated Nickel Nitride Nanoparticles as Highly Active and Durable Oxygen Evolution Electrocatalysts

[18] Chen M, Qi J, Guo D, Lei H, Zhang W and Cao R 2017 Facile synthesis of sponge-like Ni3N/NC for electrocatalytic water oxidation *Chem. Commun.* **53** 9566–9

[19] Liu X, Liu W, Ko M, Park M, Kim M G, Oh P, Chae S, Park S, Casimir A, Wu G and Cho J 2015 Metal (Ni, Co)-Metal Oxides/Graphene Nanocomposites as Multifunctional Electrocatalysts *Adv. Funct. Mater.* **25** 5799–808

[20] Gupta S, Qiao L, Zhao S, Xu H, Lin Y, Devaguptapu S V, Wang X, Swihart M T and Wu G 2016 Highly Active and Stable Graphene Tubes Decorated with FeCoNi Alloy Nanoparticles via a Template-Free Graphitization for Bifunctional Oxygen Reduction and Evolution 1–12

[21] Vij V, Sultan S, Harzandi A M, Meena A, Tiwari N, Lee W G, Yoon T and Kim K S 2017 Nickel – Based Electrocatalysts for Energy Related Applications : Oxygen Reduction , Oxygen Evolution , and Hydrogen Evolution Reactions

[22] Huang J, Sun Y, Du X, Zhang Y, Wu C and Yan C 2018 Cytomembrane-Structure-Inspired Active Ni – N – O Interface for Enhanced Oxygen Evolution Reaction **1803367** 1–8

[23] Zinn-Justin J 2021 Quantum Field Theory and Critical Phenomena: Fifth Edition *Quantum F. Theory Crit. Phenom. Fifth Ed.* 1–1049

[24] Suen N T, Hung S F, Quan Q, Zhang N, Xu Y J and Chen H M 2017 Electrocatalysis for the oxygen evolution reaction: Recent development and future perspectives *Chem. Soc. Rev.* **46** 337–65

[25] Andrew J. Mannix 2018 Borophene as a prototype for synthetic 2D materials developmen 1–26

[26] Xu Y and Ming H 2017 Electrocatalysis for the oxygen evolution reaction: recent development and future perspectives **46**

[27] Chen Z, Duan X, Wei W, Wang S and Ni B J 2019 Recent advances in transition metal-based electrocatalysts for alkaline hydrogen evolution *J. Mater. Chem. A* **7** 14971–5005

[28] Bu X, Li Y and Ho J C 2020 Efficient and stable electrocatalysts for water splitting *MRS Bull.* **45** 531–8

[29] Bu X, Li Y, Ho J C and Editors G 2021 Efficient and stable electrocatalysts for water splitting 531–8

[30] Wang S, Lu A and Zhong C J 2021 Hydrogen production from water electrolysis: role of catalysts *Nano Converg.* **8**

[31] Lee J E, Jeon K J, Show P L, Lee I H, Jung S C, Choi Y J, Rhee G H, Lin K Y A and Park Y K 2022 Mini review on H2 production from electrochemical water splitting according to special nanostructured morphology of electrocatalysts *Fuel* **308**

[32] Pathak A and Singh A K 2016 Transition Metal Nitrides: A First Principles Study *High Temp. Mater. Process.* **35** 389–98

[33] Stampfl C, Mannstadt W, Asahi R and Freeman A J 2001 Electronic structure and physical properties of early transition metal mononitrides: Density-functional theory LDA, GGA, and screened-exchange LDA FLAPW calculations *Phys. Rev. B - Condens. Matter Mater. Phys.* **63** 1–11

[34] Graeiani J, Sanz J F and Márquez A M 2009 A density functional study of initial steps in the oxidation of early transition metal nitrides, MN (M = Sc, Ti, and V) *J. Phys. Chem. C* **113** 930–8

[35] Paquin F, Rivnay J, Salleo A, Stingelin N and Silva C 2015 Multi-phase semicrystalline microstructures drive exciton dissociation in neat plastic semiconductors *J. Mater. Chem. C* **3** 10715–22

[36] Meng Z, Zheng S, Luo R, Tang H, Wang R, Zhang R, Tian T and Tang H 2022 Transition Metal Nitrides for Electrocatalytic Application: Progress and Rational Design *Nanomaterials* **12** 1–20

[37] Xie J and Xie Y 2016 Transition Metal Nitrides for Electrocatalytic Energy Conversion: Opportunities and Challenges *Chem. - A Eur. J.* **22** 3588–98

[38] Lin L, Piao S, Choi Y, Lyu L, Hong H, Kim D, Lee J, Zhang W and Piao Y 2022 Nanostructured Transition Metal Nitrides as Emerging Electrocatalysts for Water Electrolysis: Status and Challenges *EnergyChem* **4**

[39] Landon J, Demeter E, Inoğlu N, Keturakis C, Wachs I E, Vasić R, Frenkel A I and Kitchin J R 2012 Spectroscopic characterization of mixed Fe-Ni oxide electrocatalysts for the oxygen evolution reaction in alkaline electrolytes *ACS Catal.* **2** 1793–801

[40] Deng J, Zhang H, Zhang Y, Luo P, Liu L and Wang Y 2017 Striking hierarchical urchin-like peapoded NiCo 2 O 4 @ C as advanced bifunctional electrocatalyst for overall water splitting *J. Power Sources* **372** 46–53

[41] Yin Z, Chen Y, Zhao Y, Li C, Zhu C and Zhang X 2015 supercapacitors and the oxygen evolution

J. Mater. Chem. A Mater. energy Sustain. **3** 22750–8

[42] Singh R N, Awasthi R and Sinha A S K 2009 Preparation and electrochemical characterization of a new NiMoO 4 catalyst for electrochemical O 2 evolution 1613–9

[43] Singh R N, Singh J P and Singh A 2008 Electrocatalytic properties of new spinel-type MMoO 4 (M [Fe , Co and Ni) electrodes for oxygen evolution in alkaline solutions **33** 4260–4

[44] Li M, Xiong Y, Liu X, Bo X, Zhang Y, Han C and Guo L 2015 *Facile synthesis of electrospun MFe2O4 (M = Co, Ni, Cu, Mn) spinel nanofibers with excellent electrocatalytic properties for oxygen evolution and hydrogen peroxide reduction* vol 7

[45] Al-Hoshan M S, Singh J P, Al-Mayouf A M, Al-Suhybani A A and Shaddad M N 2012 Synthesis, physicochemical and electrochemical properties of nickel ferrite spinels obtained by hydrothermal method for the Oxygen Evolution Reaction (OER) *Int. J. Electrochem. Sci.* **7** 4959–73

[46] Tareen A K, Priyanga G S, Khan K, Pervaiz E, Thomas T and Yang M 2019 Nickel-Based Transition Metal Nitride Electrocatalysts for the Oxygen Evolution Reaction *ChemSusChem* **12** 3941–54

[47] Chen Q, Hou C, Wang C, Yang X and Chen Y 2018 evolution kinetics as a Pt-like electrocatalyst for water splitting † *Chem. Commun.* 3–6

[48] Zeolites T, Xu L and Sun J 2016 Recent Advances in the Synthesis and Application of **126** 444–8

[49] Manuscript A 2017 Materials Chemistry A

[50] Regier T, Wei F and Dai H 2013 An Advanced Ni − Fe Layered Double Hydroxide Electrocatalyst for Water Oxidation 2–5

[51] Mahmood N, Yao Y, Zhang J W, Pan L, Zhang X and Zou J J 2018 Electrocatalysts for Hydrogen Evolution in Alkaline Electrolytes: Mechanisms, Challenges, and Prospective Solutions *Adv. Sci.* **5**

[52] Yang Y J and Li W 2018 Ultrasonic assisted coating of multiwalled carbon nanotubes with NiFe-layered double hydroxide for improved electrocatalytic oxygen reduction *J. Electroanal. Chem.* **823** 499–504

[53] Subbaraman R, Tripkovic D, Chang K, Strmcnik D, Paulikas A P, Hirunsit P, Chan M, Greeley J, Stamenkovic V and Markovic N M 2012 Trends in activity for the water electrolyser reactions on 3d M(Ni,Co,Fe,Mn) hydr(oxy)oxide catalysts *Nat. Mater.* **11** 550–7

[54] Song F and Hu X 2014 Exfoliation of layered double hydroxides for enhanced oxygen evolution catalysis *Nat. Commun.* **5**

[55] Lu Z, Qian L, Tian Y, Li Y, Sun X and Duan X 2016 Ternary NiFeMn layered double hydroxides as highly-efficient oxygen evolution catalysts *Chem. Commun.* **52** 908–11

[56] Manuscript A 2015 Materials Chemistry A

[57] Wang Y, Xie C, Liu D, Huang X, Huo J and Wang S 2016 Nanoparticles-Stacked Porous Nickel-

Iron Nitride Nanosheet : A Highly Efficient Bifunctional Electrocatalyst for Overall Water Splitting

[58] Liu Z, Tan H, Xin J, Duan J, Su X, Hao P, Xie J, Zhan J, Zhang J, Wang J and Liu H 2018 Metallic Intermediate Phase Inducing Morphological Transformation in Thermal Nitridation : Ni 3 FeN-Based Three-Dimensional Hierarchical Electrocatalyst for Water Splitting

[59] Kamiya K, Takeuchi T, Kabeya N, Wada N, Ishimasa T, Ochiai A, Deguchi K, Imura K and Sato N K Discovery of superconductivity in quasicrystal *Nat. Commun.*

[60] Wang Y, Zhang B, Pan W, Ma H and Zhang J 2017 3 D Porous Nickel – Cobalt Nitrides Supported on Nickel Foam as Efficient Electrocatalysts for Overall Water Splitting 4170–7

[61] Xu K, Chen P, Li X, Tong Y, Ding H, Wu X, Xu K, Chen P, Li X, Tong Y, Ding H, Wu X and Chu W 2015 Metallic Nickel Nitride Nanosheets Realizing Enhanced Electrochemical Water Oxidation Metallic Nickel Nitride Nanosheets Realizing Enhanced Electrochem- ical Water Oxidation

[62] Kwag S H, Lee Y S, Lee J, Jeong D I, Kwon S Bin, Yoo J H, Woo S, Lim B S, Park W K, Kim M J, Kim J H, Lim B, Kang B K, Yang W S and Yoon D H 2019 Design of 2D Nanocrystalline Fe2Ni2N Coated onto Graphene Nanohybrid Sheets for Efficient Electrocatalytic Oxygen Evolution *ACS Appl. Energy Mater.* **2** 8502–10

[63] Guo M, Qu Y, Zeng F and Yuan C 2018 Synthetic strategy and evaluation of hierarchical nanoporous NiO/NiCoP microspheres as efficient electrocatalysts for hydrogen evolution reaction *Electrochim. Acta* **292** 88–97

[64] Mannix A J, Zhang Z, Guisinger N P, Yakobson B I and Hersam M C 2018 Borophene as a prototype for synthetic 2D materials development *Nat. Nanotechnol.* **13** 444–50

[65] Han L, Feng K and Chen Z 2017 Self-Supported Cobalt Nickel Nitride Nanowires Electrode for Overall Electrochemical Water Splitting **1** 1908–11

[66] Yang J, Shao Y, Zhang L, Huang B, Wu Y and Hao X 2018 Accepted Manuscript

[67] Lin T, Shi M, Huang F, Peng J, Bai Q, Li J and Zhai M 2018 One-Pot Synthesis of a Double-Network Hydrogel Electrolyte with Extraordinarily Excellent Mechanical Properties for a Highly Compressible and Bendable Flexible Supercapacitor *ACS Appl. Mater. Interfaces* **10** 29684–93

[68] Xing Z, Li Q, Wang D, Yang X and Sun X 2016 Self-supported nickel nitride as an efficient high-performance three-dimensional cathode for the alkaline hydrogen evolution reaction *Electrochim. Acta* **191** 841–5

[69] Zhang B, Xiao C, Xie S, Liang J, Chen X and Tang Y 2016 Iron-nickel nitride nanostructures in situ grown on surface-redox-etching nickel foam: Efficient and ultrasustainable electrocatalysts for overall water splitting *Chem. Mater.* **28** 6934–41

[70] Sun Z, Zhang J, Xie J, Zheng X, Wang M, Li X and Tang B 2018 High-performance alkaline hydrogen evolution electrocatalyzed by a Ni3N-CeO2 nanohybrid *Inorg. Chem. Front.* **5** 3042–5

[71] Wu Y, Xie Y, Niu S, Zang Y, Cai J, Bian Z, Yin X, Fang Y, Sun D, Niu D, Lu Z, Mosallanezhad A, Wang H, Rao D, Pan H and Wang G 2021 Accelerating water dissociation kinetics of Ni3N by tuning interfacial orbital coupling *Nano Res.* **14** 3458–65

[72] Yan H, Xie Y, Wu A, Cai Z, Wang L, Tian C, Zhang X and Fu H 2019 Anion-Modulated HER and OER Activities of 3D Ni–V-Based Interstitial Compound Heterojunctions for High-Efficiency and Stable Overall Water Splitting *Adv. Mater.* **31** 1–9

[73] Zhou P, Zhai G, Lv X, Liu Y, Wang Z, Wang P, Zheng Z, Cheng H, Dai Y and Huang B 2021 Boosting the electrocatalytic HER performance of Ni3N-V2O3 via the interface coupling effect *Appl. Catal. B Environ.* **283** 119590

[74] Electrocatalysts H, Zhang Y, Ouyang B, Xu J, Chen S, Rawat R S and Fan H J 2016 3D Porous Hierarchical Nickel – Molybdenum Nitrides Synthesized by RF Plasma as Highly Active and Stable 1–6

[75] Hua W, Sun H, Liu H, Li Y and Wang J G 2021 Interface engineered NiMoN/Ni3N heterostructures for enhanced alkaline hydrogen evolution reaction *Appl. Surf. Sci.* **540** 148407

[76] Li J, Zhu Z, Huang Y, Wang F and Balogun M S (Jie T 2022 Ni3N: A multifunctional material for energy storage and electrocatalysis *Mater. Today Energy* **26**

[77] Shalom M, Ressnig D, Yang X, Clavel G, Fellinger T P and Antonietti M 2015 Nickel nitride as an efficient electrocatalyst for water splitting *J. Mater. Chem. A* **3** 8171–7

[78] Liu B, He B, Peng H Q, Zhao Y, Cheng J, Xia J, Shen J, Ng T W, Meng X, Lee C S and Zhang W 2018 Unconventional Nickel Nitride Enriched with Nitrogen Vacancies as a High-Efficiency Electrocatalyst for Hydrogen Evolution *Adv. Sci.* **5** 1–7

[79] Theerthagiri J, Lee S J, Murthy A P, Madhavan J and Choi M Y 2020 Fundamental aspects and recent advances in transition metal nitrides as electrocatalysts for hydrogen evolution reaction: A review *Curr. Opin. Solid State Mater. Sci.* **24** 100805

[80] Luo X, Ma H, Gao J, Yu L, Gu X and Liu J 2022 Nickel-Rich Ni3N Particles Stimulated by Defective Graphitic Carbon Nitrides for the Effective Oxygen Evolution Reaction *Ind. Eng. Chem. Res.* **61** 2081–90

[81] Gao X, Liu X, Zang W, Dong H, Pang Y, Kou Z, Wang P, Pan Z, Wei S, Mu S and Wang J 2020 Synergizing in-grown Ni3N/Ni heterostructured core and ultrathin Ni3N surface shell enables self-adaptive surface reconfiguration and efficient oxygen evolution reaction *Nano Energy* **78** 105355

[82] Yang Y, Jin X, Zhan F and Yang Y 2024 Enhancing the electronic structure of Ni-based electrocatalysts through N element substitution for the hydrogen evolution reaction *Nanoscale* **16**

11604–9

[83] Hu Y W, Sultana F, Balogun M S, Xiong T, Huang Y and Xia Y 2024 Bi-cation incorporated Ni3N nanosheets boost water dissociation kinetics for enhanced alkaline hydrogen evolution activity *Nanoscale* **16** 4325–32

[84] Zhang D, Li H, Riaz A, Sharma A, Liang W, Wang Y, Chen H, Vora K, Yan D, Su Z, Tricoli A, Zhao C, Beck F J, Reuter K, Catchpole K and Karuturi S 2022 Unconventional direct synthesis of Ni3N/Ni with N-vacancies for efficient and stable hydrogen evolution *Energy Environ. Sci.* **15** 185–95

[85] Dev P, Xue Y and Zhang P 2008 Defect-induced intrinsic magnetism in wide-gap III nitrides *Phys. Rev. Lett.* **100** 1–4

[86] Stoeva Z, Smith R I and Gregory D H 2006 Stoichiometry and defect structure control in the ternary lithium nitridometalates Li3-x-yNixN *Chem. Mater.* **18** 313–20

[87] S. Anjum Characterization of Nickel Nitride and Nitrogen-Doped Carbon in Magnetron Sputtering _ Elicit

[88] Jiawei Guo 2023 Hierarchical porous 3D Ni3N-CoN_NC heterojunction nanosheets with nitrogen vacancies for high-performance flexible supercapacitor - ScienceDirect

[89] Shen Z, Zhang Z, Li M, Yuan Y, Zhao Y, Zhang S, Zhong C, Zhu J, Lu J and Zhang H 2020 Rational Design of a Ni3N0.85Electrocatalyst to Accelerate Polysulfide Conversion in Lithium-Sulfur Batteries *ACS Nano* **14** 6673–82

[90] Song F, Li W, Yang J, Han G, Liao P and Sun Y 2018 Interfacing nickel nitride and nickel boosts both electrocatalytic hydrogen evolution and oxidation reactions *Nat. Commun.* **9**

[91] Ni W, Krammer A, Hsu C S, Chen H M, Schüler A and Hu X 2019 Ni3N as an Active Hydrogen Oxidation Reaction Catalyst in Alkaline Medium *Angew. Chemie - Int. Ed.* **58** 7445–9

[92] Purcel M, Müller A S, Diehl P, Kappis K, Trunschke A and Muhler M 2024 Long-Term Stability of Ammonia Decomposition over Nickel-Based Catalysts *Energy Technol.*

[93] Zhang W, Rafiq M, Lu J, Woldu A R, Zhou J, Xia H, Chu P K, Hu L and Lu F 2023 Durable Ni3N porous nanosheets array for non-noble metal methanol oxidation reaction *APL Mater.* **11**

[94] Ma K Y, Kim H, Hwang H, Jeong D S, Lee H J, Cho K, Yang J, Jeong H Y and Shin H S 2024 Enhanced Long-Term Stability of Crystalline Nickel–Boride (Ni23B6) Electrocatalyst by Encapsulation with Hexagonal Boron Nitride *Adv. Sci.* **2403674** 1–7

[95] Lee S Y, Kim I S, Cho H S, Kim C H and Lee Y K 2021 Resolving Potential-Dependent Degradation of Electrodeposited Ni(OH)2 Catalysts in Alkaline Oxygen Evolution Reaction (OER): In Situ XANES Studies *Appl. Catal. B Environ.* **284** 119729

[96] Kreider M E, Gallo A, Back S, Liu Y, Siahrostami S, Nordlund D, Sinclair R, Nørskov J K, King

L A and Jaramillo T F 2019 Precious Metal-Free Nickel Nitride Catalyst for the Oxygen Reduction Reaction *ACS Appl. Mater. Interfaces* **11** 26863–71

[97] Spöri C, Kwan J T H, Bonakdarpour A, Wilkinson D P and Strasser P 2017 The Stability Challenges of Oxygen Evolving Catalysts: Towards a Common Fundamental Understanding and Mitigation of Catalyst Degradation *Angew. Chemie - Int. Ed.* **56** 5994–6021

[98] Meng X, Zhao X, Min Y, Xu Q, Li Q and Cai W 2024 Oxygen vacancy-enhanced Ni3FeN/NF nanoparticle catalysts for efficient and stable electrolytic water splitting *Electrochim. Acta* **497**

[99] Rossetti N, Ugolotti A, Cometto C, Celorrio V, Dražić G, Di Valentin C and Calvillo L 2024 Insights into the active nickel centers embedded in graphitic carbon nitride for the oxygen evolution reaction *J. Mater. Chem. A* **12** 6652–62

[100] Shalom M, Ressnig D, Yang X, Clavel G, Fellinger T P and Antonietti M 2015 Nickel nitride as an efficient electrocatalyst for water splitting *J. Mater. Chem. A* **3** 8171–7

[101] J. Thambiliyagodage C, Hakat Y and G. Bakker M 2016 One Pot Synthesis of Carbon/Ni Nanoparticle Monolithic Composites by Nanocasting and Their Catalytic Activity for 4-Nitrophenol Reduction *Curr. Catal.* **5** 135–46

[102] Wen Z, Ci S, Hou Y and Chen J 2014 Facile one-pot, one-step synthesis of a carbon nanoarchitecture for an advanced multifunctonal electrocatalyst *Angew. Chemie - Int. Ed.* **53** 6496–500

[103] Wang Y, Wang X, Antonietti M and Zhang Y 2010 Facile one-pot synthesis of nanoporous carbon nitride solids by using soft templates *ChemSusChem* **3** 435–9

[104] Paraknowitsch J P, Sukhbat O, Zhang Y and Thomas A 2012 One-pot synthesis of metal-doped mesoporous materials from (dicyanamido)metallate precursors *Eur. J. Inorg. Chem.* 4105–16

[105] Jiang H, Gu J, Zheng X, Liu M, Qiu X, Wang L, Li W, Chen Z, Ji X and Li J 2019 Defect-rich and ultrathin N doped carbon nanosheets as advanced trifunctional metal-free electrocatalysts for the ORR, OER and HER *Energy Environ. Sci.* **12** 322–33

[106] Maślana K, Kaleńczuk R J, Zielińska B and Mijowska E 2020 Synthesis and characterization of nitrogen-doped carbon nanotubes derived from g-C3N4 *Materials (Basel).* **13**

[107] Luo Q, Lu C, Liu L and Zhu M 2023 Triethanolamine assisted synthesis of bimetallic nickel cobalt nitride/nitrogen-doped carbon hollow nanoflowers for supercapacitor *Microstructures* **3**

[108] Iwasaki T, Tomisawa M, Yoshimura T, Nakamura H, Ohyama M, Asao K and Watano S 2015 Synthesis of nitrogen-doped carbon nanocoils with adjustable morphology using ni-fe layered double hydroxides as catalyst precursors *Nanomater. Nanotechnol.* **5** 1–7

[109] Wu G and Zelenay P 2013 Nanostructured nonprecious metal catalysts for oxygen reduction reaction *Acc. Chem. Res.* **46** 1878–89

[110] Fan H, Yu H, Zhang Y, Zheng Y, Luo Y, Dai Z, Li B, Zong Y and Yan Q 2017 Fe-Doped Ni3C Nanodots in N-Doped Carbon Nanosheets for Efficient Hydrogen-Evolution and Oxygen-Evolution Electrocatalysis *Angew. Chemie - Int. Ed.* **56** 12566–70

[111] Li X H and Antonietti M 2013 Metal nanoparticles at mesoporous N-doped carbons and carbon nitrides: Functional mott–schottky heterojunctions for catalysis *Chem. Soc. Rev.* **42** 6593–604

[112] Muñoz-Sandoval E, Fajardo-Díaz J L, Sánchez-Salas R, Cortés-López A J and López-Urías F 2018 Two Sprayer CVD Synthesis of Nitrogen-doped Carbon Sponge-type Nanomaterials *Sci. Rep.* **8** 1–14

[113] Nishchakova A D, Bulushev D A, Trubina S V., Stonkus O A, Shubin Y V., Asanov I P, Kriventsov V V., Okotrub A V. and Bulusheva L G 2023 Highly Dispersed Ni on Nitrogen-Doped Carbon for Stable and Selective Hydrogen Generation from Gaseous Formic Acid *Nanomaterials* **13**

[114] Pacuła A, Drelinkiewicz A, Ruggiero-Mikołajczyk M, Pietrzyk P, Socha R P, Krzan M, Nattich-Rak M, Duraczyńska D, Bielańska E and Zimowska M 2022 N-doped carbon materials produced by CVD with the compounds derived from LDHs *J. Mater. Sci.* **57** 18298–322

[115] Li J, Yin C, Wang S, Zhang B and Feng L 2024 Built-in electrophilic/nucleophilic domain of nitrogen-doped carbon nanofiber-confined Ni2P/Ni3N nanoparticles for efficient urea-containing water-splitting reactions *Chem. Sci.* **15** 13659–67

[116] Demazeau G, Goglio G, Largeteau A, Demazeau G, Goglio G and Largeteau A 2021 Solvothermal processes and the synthesis of nitrides To cite this version : HAL Id : hal-00348842

[117] Peera S G, Koutavarapu R, Liu C, Rajeshkhanna G, Asokan A and Reddy C V 2021 Cobalt Nanoparticle-Embedded Nitrogen-Doped Carbon Catalyst Derived from a Solid-State Metal-Organic Framework Complex for OER and HER Electrocatalysis *Energies* **14** 1320

[118] Li J 2022 *Oxygen Evolution Reaction in Energy Conversion and Storage: Design Strategies Under and Beyond the Energy Scaling Relationship* vol 14 (Springer Nature Singapore)

[119] Seok S 2021 Ni Nanoparticles on Ni Core_N-Doped Carbon Shell Heterostructures for Electrocatalytic Oxygen Evolution _ ACS Applied Nano Materials

[120] Zhang X, Huang L, Han Y, Xu M and Dong S 2017 Nitrogen-doped carbon encapsulating γ - MoC / Ni heterostructures

[121] Ye Y, Zhou G, Li K and Tong Y 2023 Dual-Modification Engineering of CoNi Alloy Realizing Robust Performance for Electrocatalytic Hydrogen Production *Catalysts* **13**

[122] Saha S and Ganguli A K 2017 FeCoNi Alloy as Noble Metal-Free Electrocatalyst for Oxygen Evolution Reaction (OER) *ChemistrySelect* **2** 1630–6

[123] Negahdar L, Zeng F, Palkovits S, Broicher C and Palkovits R 2019 Mechanistic Aspects of the

Electrocatalytic Oxygen Evolution Reaction over Ni−Co Oxides *ChemElectroChem* **6** 5588–95

[124] Zhao M 2022 Bimetal Mo–Ni_NC as an effective electrocatalyst with accelerated kinetics for the oxygen evolution reaction - ScienceDirect

[125] Liu J 2022 Advances in Noble Metal-Free Electrocatalysts for OER _ Elicit

[126] Yuan Y, Sun L, Li Y, Zhan W, Wang X and Han X 2020 Synergistic Modulation of Active Sites and Charge Transport: N/S Co-doped C Encapsulated NiCo2O4/NiO Hollow Microrods for Boosting Oxygen Evolution Catalysis *Inorg. Chem.* **59** 4080–9

[127] Zhong G, Li S, Xu S, Liao W, Fu X and Peng F 2018 Nickel Nanoparticles Encapsulated in Nitrogen-Doped Carbon Nanotubes as Excellent Bifunctional Oxygen Electrode for Fuel Cell and Metal-Air Battery *ACS Sustain. Chem. Eng.* **6** 15108–18

[128] Zou R, Xu M, He S A, Han X, Lin R, Cui Z, He G, Brett D J L, Guo Z X, Hu J and Parkin I P 2018 Cobalt nickel nitride coated by a thin carbon layer anchoring on nitrogen-doped carbon nanotube anodes for high-performance lithium-ion batteries *J. Mater. Chem. A* **6** 19853–62

[129] Ding J, Ji S, Wang H, Linkov V, Gai H, Liu F, Liu Q and Wang R 2019 N-Doped 3D Porous Ni/C Bifunctional Electrocatalysts for Alkaline Water Electrolysis *ACS Sustain. Chem. Eng.* **7** 3974–81

[130] Wu Z P, Lu X F, Zang S Q and Lou X W 2020 Non-Noble-Metal-Based Electrocatalysts toward the Oxygen Evolution Reaction *Adv. Funct. Mater.* **30**

[131] Brewster D A, Koch M D and Knowles K E 2021 Evaluation of electrochemical properties of nanostructured metal oxide electrodes immersed in redox-inactive organic media *Phys. Chem. Chem. Phys.* **23** 17904–16

[132] Malkow T, Pilenga A and Tsotridis G 2018 *EU harmonised test procedure: electrochemical impedance spectroscopy for water electrolysis cells*

[133] Chukwuneke C E, Kawashima K, Li H, Marquez R A, Son Y J, Smith L A, Celio H, Henkelman G and Mullins C B 2023 Electrochemically engineered domain: nickel-hydroxide/nickel nitride composite for alkaline HER electrocatalysis *J. Mater. Chem. A* **12** 1654–61

[134] Yu L, Zhu Q, Song S, McElhenny B, Wang D, Wu C, Qin Z, Bao J, Yu Y, Chen S and Ren Z 2019 Non-noble metal-nitride based electrocatalysts for high-performance alkaline seawater electrolysis *Nat. Commun.* **10** 1–10

[135] Sahiner M, Demirci S and Sahiner N 2024 Polydopamine Coating of Graphitic Carbon Nitride, g-C3N4, Improves Biomedical Application *Biomedicines* **12** 1–17

[136] Atamanov M, Lyu J Y, Chen S and Yan Q L 2021 Preparation of CNTs Coated with Polydopamine-Ni Complexes and Their Catalytic Effects on the Decomposition of CL-20 *ACS Omega* **6** 22866–75

[137] Kim Y and Kim J 2020 Carbonization of polydopamine-coating layers on boron nitride for thermal conductivity enhancement in hybrid polyvinyl alcohol (PVA) composites *Polymers (Basel).* **12**

[138] Domonov D P, Pechenyuk S I, Belyaevskii A T and Yusenko K V. 2020 Formation of nanostructured carbon from [ni(Nh3)6]3[fe(cn)6]2 *Nanomaterials* **10**

[139] De B S, Kumar P, Khare N, Luo J L, Elias A and Basu S 2021 Microfabrication of the Ammonia Plasma-Activated Nickel Nitride-Nickel Thin Film for Overall Water Splitting in the Microfluidic Membraneless Electrolyzer *ACS Appl. Energy Mater.* **4** 9639–52

[140] Tsai T Y and Chen W Y 2022 The Effect of Up-Flow Rate on the Nitrogen Treatment Efficiency and Sludge Characteristics of ANAMMOX Process with Up-Flow Anaerobic Sludge Bed Reactor *Sustain.* **14**

[141] Tiruneh S N, Kang B K, Choi H W, Kwon S Bin, Kim M S and Yoon D H 2018 Millerite Core–Nitrogen-Doped Carbon Hollow Shell Structure for Electrochemical Energy Storage *Small* **14** 1–10

[142] Soo Kang J, Park M A, Kim J Y, Ha Park S, Young Chung D, Yu S H, Kim J, Park J, Choi J W, Jae Lee K, Jeong J, Jae Ko M, Ahn K S and Sung Y E 2015 Reactively sputtered nickel nitride as electrocatalytic counter electrode for dye- and quantum dot-sensitized solar cells *Sci. Rep.* **5** 1–11

[143] Shanker G S and Ogale S 2021 Faceted Colloidal Metallic Ni3N Nanocrystals: Size-Controlled Solution-Phase Synthesis and Electrochemical Overall Water Splitting *ACS Appl. Energy Mater.* **4** 2165–73

[144] Wang G, Sun Y, Li D, Liang H W, Dong R, Feng X and Müllen K 2015 Controlled Synthesis of N-Doped Carbon Nanospheres with Tailored Mesopores through Self-Assembly of Colloidal Silica *Angew. Chemie - Int. Ed.* **54** 15191–6

[145] Kawashima K, Márquez-Montes R A, Li H, Shin K, Cao C L, Vo K M, Son Y J, Wygant B R, Chunangad A, Youn D H, Henkelman G, Ramos-Sánchez V H and Mullins C B 2021 Electrochemical behavior of a Ni3N OER precatalyst in Fe-purified alkaline media: The impact of self-oxidation and Fe incorporation *Mater. Adv.* **2** 2299–309

[146] Chen G, Wang T, Zhang J, Liu P, Sun H, Zhuang X, Chen M and Feng X 2018 Accelerated Hydrogen Evolution Kinetics on NiFe-Layered Double Hydroxide Electrocatalysts by Tailoring Water Dissociation Active Sites *Adv. Mater.* **30** 1–7

[147] Zhuang Z, Sheng W and Yan Y 2014 Synthesis of Monodispere Au @ Co 3 O 4 Core-Shell Nanocrystals and Their Enhanced Catalytic Activity for Oxygen Evolution Reaction 1–6

[148] Wang X, Kolen'Ko Y V. and Liu L 2015 Direct solvothermal phosphorization of nickel foam to fabricate integrated Ni2P-nanorods/Ni electrodes for efficient electrocatalytic hydrogen evolution

Chem. Commun. **51** 6738–41